AN EXPERIMENTAL INVESTIGATION OF LOW TEMPERATURE FLUORESCENCE IN SAPPHIRE

By

JOEL DEAN BREWER

Bachelor of Science

Oklahoma State University

Stillwater, Oklahoma

1978

Submitted to the Faculty of the Graduate College
of the Oklahoma State University
in partial fulfillment of the requirements
for the Degree of
MASTER OF SCIENCE
December, 1979

AN EXPERIMENTAL INVESTIGATION OF

LOW TEMPERATURE FLUORESCENCE

IN SAPPHIRE

Thesis Approved:

Geo P Burns

J G Martin

R. C. Powell

Norman N Durham

Dean of the Graduate College

ACKNOWLEDGMENTS

The author wishes to thank his major adviser, Dr. Geoffrey P. Summers, for his enlightening discussions and helpful guidance throughout the research which led to this thesis.

Thanks is given to the Department of Energy whose financial support helped to make this research possible.

Thanks is also given to the Physics Faculty of Oklahoma State University for their excellent instruction, to Bryce Jeffries for his helpful advice and to Janet Sallee for her excellence and efficiency in typing this thesis.

A special thanks is given to my wife, Becky, for her patience and understanding throughout the development of this project.

TABLE OF CONTENTS

LIST OF TABLES

LIST OF FIGURES

CHAPTER I

INTRODUCTION

The single crystal sapphire, α-Al_2O_3, possesses a unique combination of physical, mechanical, and chemical properties which make it useful in widely diversified applications. Some of these properties are listed in Table I. Applications for single crystal sapphires include: infrared windows and lenses, detector cell windows and lenses, spectrometer windows, optical filter substrates, microcircuit substrates, thin film substrates, wear pads, solar cell protective covers, cryogenic heat sinks, laser reflectors, magnetic tape guides and cutters, photomultiplier tubes and pressure cell windows. The subject of this paper is an experimental study of the electronic structure of a simple defect in α-Al_2O_3. This defect is the F-center (i.e., two electrons trapped at an oxygen ion vacancy). In order to understand this defect it is important to investigate the crystalline structure of Al_2O_3 and the local symmetry structure of the F-center.

Corendum, i.e., single crystal α-aluminum oxide, is classed as a rhombohedral structure. Indexing though is usually done on hexagonal axes. The structure is shown in Figure 1. From this it is seen that the cell structure is hexagonal consisting of an equilateral triangle of oxygen atoms above and below an aluminum atom, the two triangles being rotated 60° with respect to each other. The aluminum ion appears to be in the center of the two triangles but in reality it is slightly

TABLE I

LIST OF Al_2O_3 PROPERTIES

Properties	Values[a]
Molecular Weight	101.94
Crystal Class	Hexagonal system - rhombohedral class
Specific Gravity	3.98
Hardness	Moh 9 - Knoop 1525-2000 depending on orientation (1000 gram indenter)
Bulk Modulus	300,000 psi
Young's Modulus	Angle indicated is that between the C-axis and the axis of the bar: 30° - 5.5 x 10^7 psi; 45° - 5.1 x 10^7 psi 60° - 5.0 x 10^7 psi; 75° - 5.6 x 10^7 psi
Modulus of Rigidity	2.15 x 10^7 psi (minimum)
Melting Temperature	2.040 ± 10°C
Specific Heat	0.0249 @ 91K; 0.1813 @ 291K
Thermal Conductivity	Temperature — Thermal Conductivity (cal./cm.sec. $^{\circ}$C) 2.5K — 0.08 4.2K — 0.28 20K — 8.4 35K — 16.0 77K — 2.3 200K — 0.21
Heat Capacity	Temperature — Heat Capacity (Abs. Joules/Deg.Mole) 50K — 2 100K — 13 200K — 52 300K — 79

TABLE I (Continued)

Properties	Values[a]	
Optical Transmission	Wavelength (microns)	Transmittance of 1 mm Plate
	0.28	79%
	0.22	72%
	0.20	66%
	0.18	53%
Volume Resistivity	$500^{\circ}C$ - 10^{11} ohm/cm	
	$1000^{\circ}C$ - 10^{9} ohm/cm	
	$1500^{\circ}C$ - 10^{5} ohm/cm	
Dielectric Constant	Temperature	Electric Field Relative to C-axis:
		Perpendicular / Parallel
	$20^{\circ}C$	9.35 / 11.53
	$100^{\circ}C$	9.43 / 11.66
	$300^{\circ}C$	9.66 / 12.07
	$500^{\circ}C$	9.92 / 12.54

[a]Reference 1.

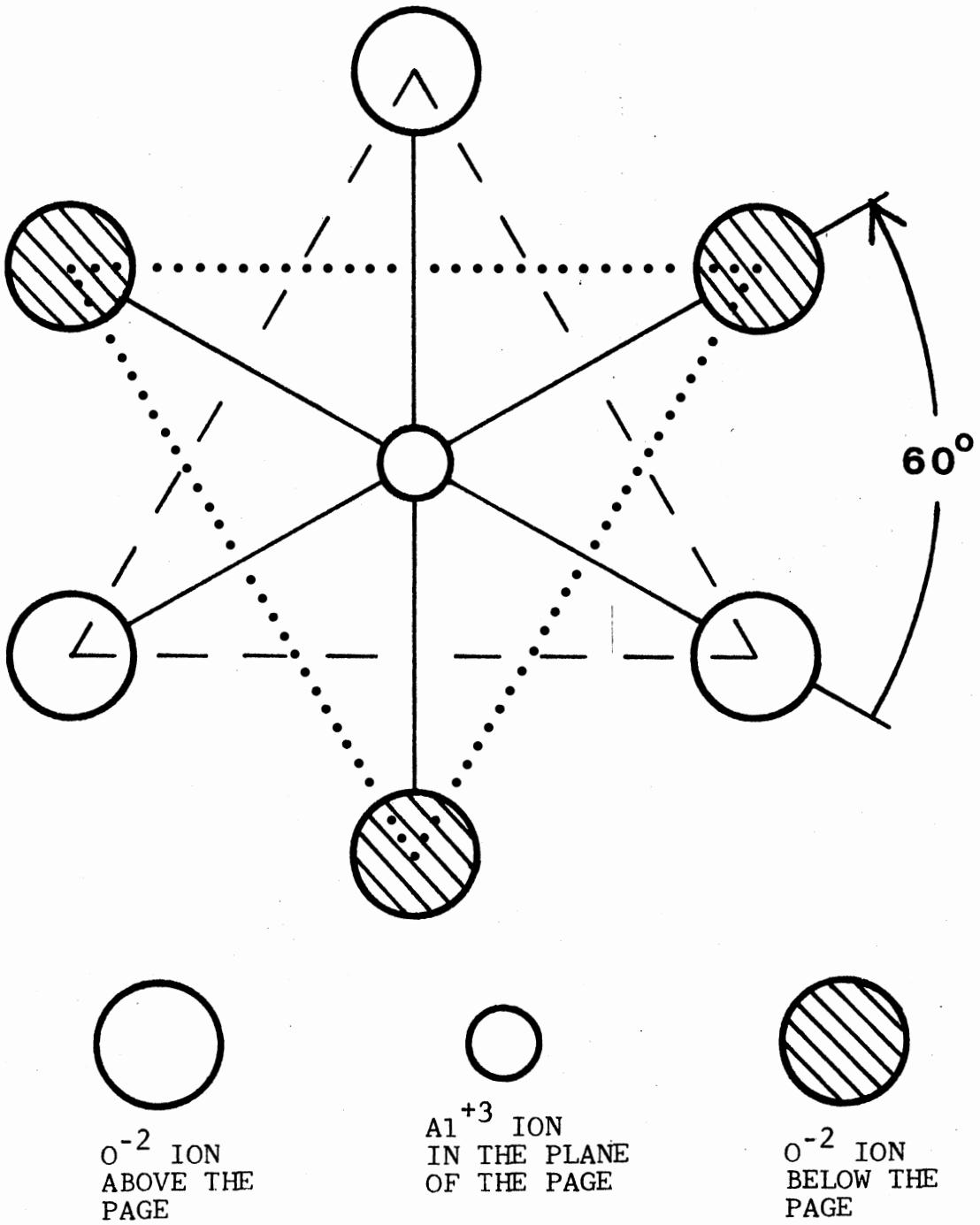

Figure 1. Structure of α-Al_2O_3

displaced. The cell then has C_{3v} symmetry while the crystal only has C_3 symmetry.

Simple defects occur when an O^{-2} ion or an Al^{+3} ion is removed. This results in F-type or V-type centers, respectively. F-type centers can be produced in several ways in sapphire. Two ways are by using either particle irradiation or by growing the crystal in a reducing atmosphere. The crystals under consideration here were grown in the usual way which means in an atmosphere of argon or under a vacuum. These crystals are therefore, grown under a reducing atmosphere.

The F-center's nearest neighbors are indicated in Figure 2. The bond lengths indicate the shortest Al-O and longest Al-O distances in the cell discussed earlier. It is seen in Figure 2 that the F-center has C_2 symmetry compared to the crystal symmetry of C_3.

Both F and F^+ centers are thought to be present in sapphire. An F- center results if an O^{-2} vacancy captures two electrons and an F^+ center results if only one electron is captured. The F and F^+ centers in other materials such as the alkaline earth oxides can be associated with certain absorption and emission bands. In sapphire it has taken considerable research to assign certain absorption and emission bands to the F-type centers. It is usual in defect center research to identify optical absorption bands by correlating their behavior with the behavior of e.s.r. absorptions observed in the same samples. In sapphire, however, no e.s.r. signal has satisfactorily been identified for any anion vacancy center. So identification of the F bands and the F^+ bands has been more difficult.

The identifications have had to be made by indirect means and by analogy with known F-type center behavior in the alkaline earth oxides.

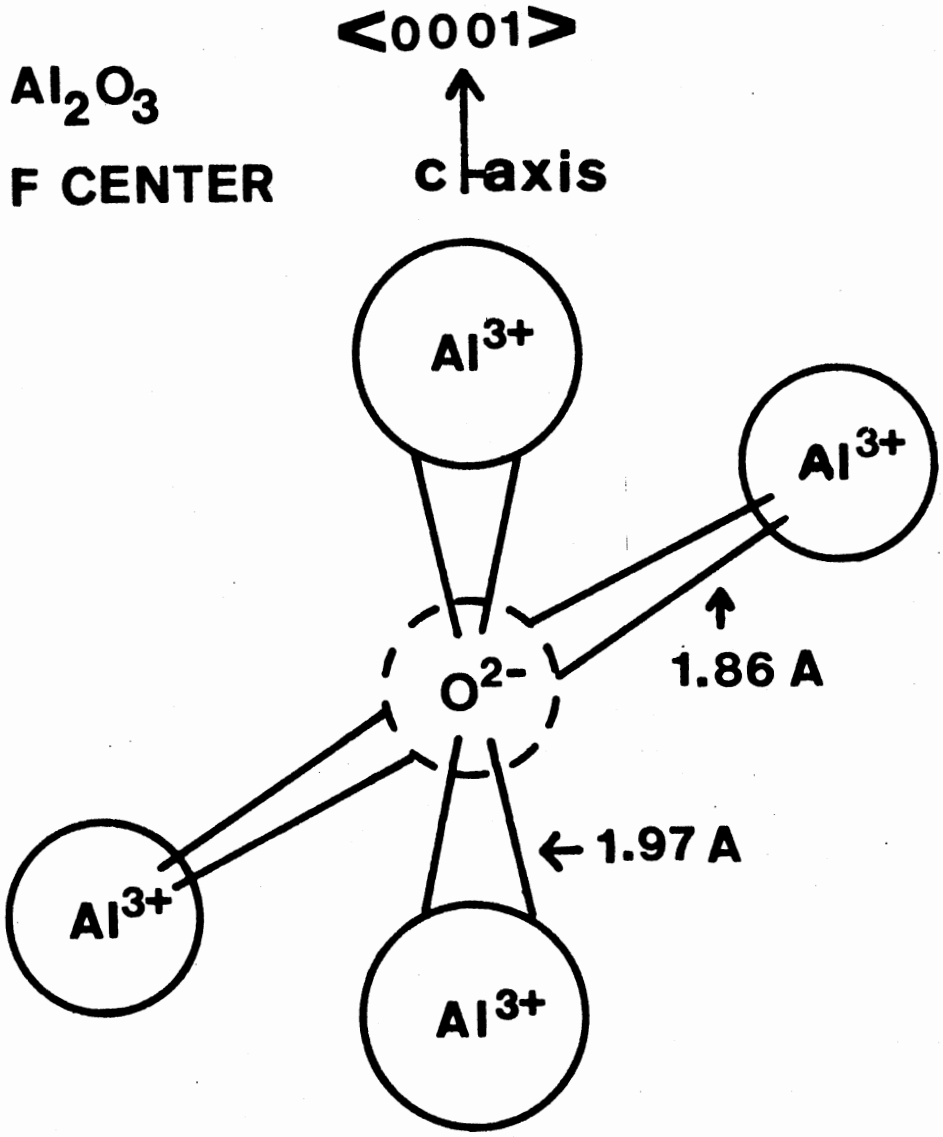

Figure 2. Structure of the F-center in α-Al_2O_3

In these oxides knock on damage is in the form of intrinsic, structural damage. An early experiment that demonstrates that this is also what happens in sapphire was conducted by Arnold and Compton (2). They found that for an incident electron energy of 0.37 MeV or greater an absorption band at 6.1 eV was created. The displacement energy calculated from the data of the knock on damage experiments was 50 eV if an Al^{+3} ion was assumed to have been displaced or 90 eV if an O^{-2} ion was assumed to have been displaced.

Arnold and Compton were unable to determine, however, which ion was being displaced. A series of experiments by Pells (3) utilizing ion beam irradiation helps in identifying which is actually displaced. In this series of experiments sapphire samples were irradiated with 3.0 MeV H^{+}, 3.0 MeV N^{+}, 2.4 MeV O^{+} and fast neutrons. In all of the experiments except for the one using O^{+}, a large absorption band around 6.1 eV and a smaller absorption band around 4.8 eV was observed. In the O^{+} irradiated sample no comparable absorption band was found over the range of 200 nm to 350 nm. It is known that if the knock on damage source is the same as what is to be the target of the damage, little or no damage to the sample will be detected. If the 6.1 eV absorption band were due to an oxygen vacancy then the lack of this band in the O^{+} irradiated sample could be accounted for and the oxygen atom could be assigned to the defect observed in the experiments by Arnold and Compton. In fact the suggested assignment is supported by bleaching experiments conducted by Turner and Crawford.

The first of Turner and Crawford's (4) bleaching experiments to be reviewed in this thesis is one done on an γ-irradiated sapphire. It showed a 410 and a 227 nm absorption band plus an OH band at 3316 cm^{-1}.

It was found that bleaching into either the 410 or 227 nm bands resulted in a reduction of intensity in both of these bands. Bleaching at 410 nm was found to completely remove the 227 nm band out bleaching the 227 nm band was found to reduce the intensity of the 410 nm band to one third of its original value even after the 227 nm band was completely eliminated. Turner and Crawford concluded that the 410 nm band was a composite V band, one component being a V_{OH}^{-} center (trapped hole). The 227 nm band was found to be due to Cr^{+2} which was formed during the irradiation when Cr^{+3} captured an electron.

Turner and Crawford (5) in a later experiment utilized the 410 nm V band to demonstrate that the 6.1 eV absorption band was due to an oxygen vacancy. They used the reasoning that if upon excitation into the 3.0 eV (410 nm) band it was found that either the 6.1 eV band did not change or increase in amplitude then the defect must be due to a hole. If upon bleaching with 3.0 eV light the 6.1 eV band decreased in intensity then it can be concluded that the 6.1 eV band is due to a trapped electron. When the experiment was carried out it was found that the 6.1 eV band was substantially reduced, therefore the 6.1 eV band is due to a trapped electron center.

With the 6.1 eV band established as due to an F-type center it is still not determined whether it is an F or an F^{+}-center. It is known that if an Al_2O_3 crystal is irradiated in a nuclear reactor several absorption bands appear, these are at 6.02 eV, 5.34 eV, 4.84 eV, 4.21 eV, 3.74 eV, 2.64 eV, and 2.00 eV, where the 6.02 eV band is the previously mentioned 6.1 eV band. The 5.34 eV band is referred to as a 5.4 eV band and the 4.84 eV band is referred to as the 4.8 eV band.

Utilizing the presence of these bands Lee and Crawford (6) were

able to perform bleaching experiments which supplied information on what type of F center produced the 6.1 eV band. They observed that irradiating the sample with 6.1 eV light caused the 4.8 eV and 5.4 eV absorption bands to be enhanced. Bleaching with 6.1 eV light also greatly increased an emission band at 3.8 eV. If it is assumed that the 6.1 eV band is an F-center it can then be concluded that what is happening is that an electron is being removed from an F-center leaving behind an F^+-center. This leads to the assignment of the 4.8 and 5.4 eV absorption bands to the F^+-center. The 6.1 eV absorption band and its related 3.0 eV emission band is 'often' assigned to an F-center.

Similar bleaching experiments by Draeger and Summers (7) on growth colored sapphires showing the 6.1 eV band behaved the same way in these samples. It was also shown that the 3.0 eV emission had an excitation spectrum similar to the 6.1 eV absorption band.

The assignments made above as to the origin of certain absorption bands are supported further by experimental work by La, Bartran, and Cox (8).

They calculated an energy level scheme for the F^+-center in Al_2O_3 using a point-ion model. The energy level scheme they predicted is shown in Figure 3 where the energies indicated are from experiment, not theory. The 1A state is similar to a 1s state in a model with spherical symmetry. The upper three levels are derived from the triple degeneracy of a 2p state. The 2p state is split into a 1B, 2A, and 2B by the C_2 crystalline field.

As indicated, the energies in Figure 3 are experimentally determined. This was done by Evans and Stapelbrock (9). They used a 14-Mev neutron irradiated high-purity crystalline Al_2O_3 in experiments which

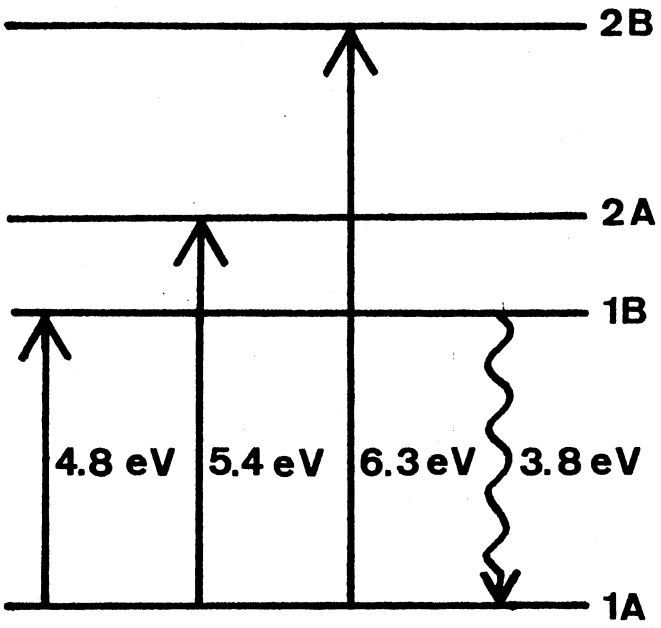

Figure 3. Energy Level Scheme for the F^+-Center

enabled them to assign the 4.8 eV and 5.4 eV absorption bands to the 1A to 1B and 1A to 2A transitions, respectively. Also the 3.8 eV luminescence emission of the F^+-center was assigned to the 1B to 1A transition. The 1A to 2B absorption was tentatively assigned to an absorption band at about 6.3 eV. This puts the levels in an order which is in agreement with that predicted by La, Bartram, and Cox. La, Bartram, and Cox did predict energies for the levels but these values did not agree with the experimentally determined values. It is not unusual for this to occur when point-ion calculations are used. The fact that theoretical calculation of the energy level scheme agrees with experiment indicates that the assignment of the 4.8 eV and 5.4 eV absorption band to the F^+-center by means of the bleaching experiments was probably correct. Therefore the assignment of the 6.1 eV band and its related emission at 3.0 eV is also confirmed.

Three of the four samples used in the experiments here were growth colored, the other was irradiated with fast neutrons. It can be seen in Figures 4 and 5 that all four samples contain the 6.1 eV absorption band.

The research done to date on the F-center 3.0 eV fluorescence emission is for temperatures of 77K and above. Lee and Crawford (10) have reported a lifetime of 36 msec for this emission in an additively colored sample at a temperature of 77K while Lehmann and Gunthard (11) have reported a lifetime of 40 msec between 77K and 300K for the same type of crystal. Lehmann and Gunthard also observed an additional long-lived phosphorescence near room temperature.

No published data exists for the behavior of the 3.0 eV emission below 77K. The purpose of this thesis is to investigate the fluores-

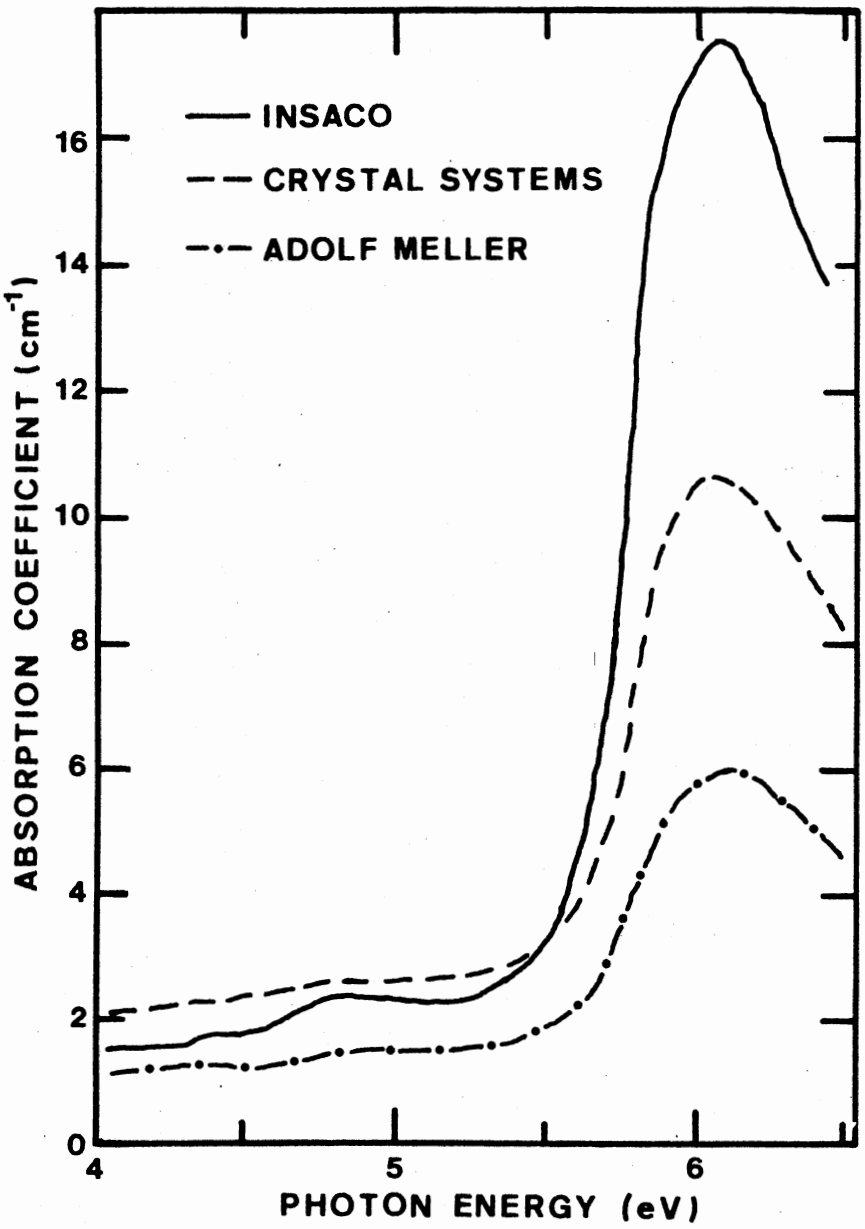

Figure 4. Absorption Coefficients for the Insaco, Crystal Systems, and Adolf Meller Samples

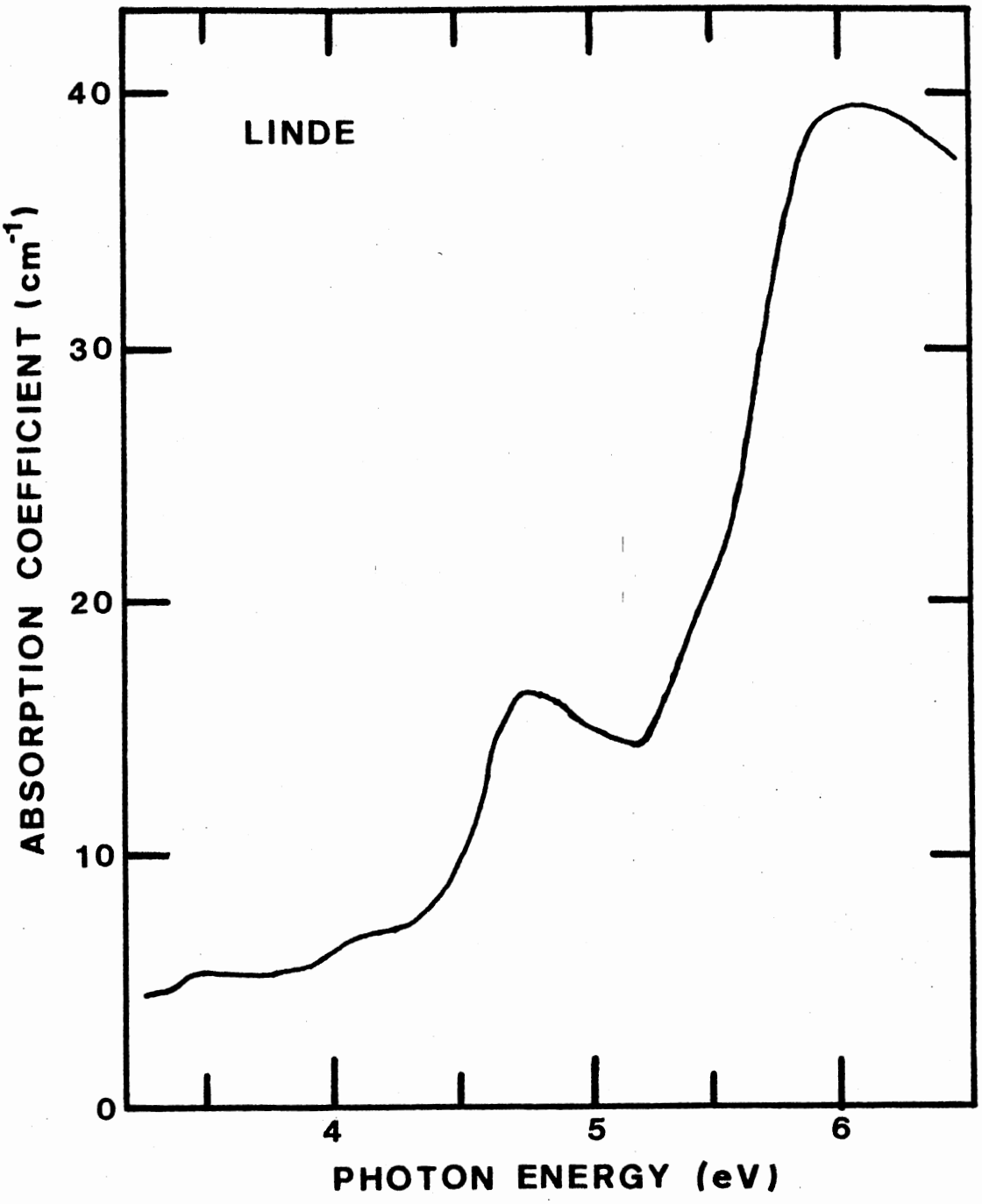

Figure 5. Absorption Coefficient for the Linde Sample

cence emission from about 4K to 300K. The analysis of the data from this investigation will then be related to an electronic structure for the F-center which is tentatively proposed to describe the experimental results. The long-lived phosphorescence observed near room temperature by Lehmann and Gunthard (11) will also be investigated.

CHAPTER II

EXPERIMENTAL APPARATUS AND PROCEDURE

Introduction

Several types of measurements are reported in this thesis. These include:

1) Fluorescence lifetime measurements,

2) Polarization measurements,

3) Phosphorescence lifetime measurements,

4) Photoconductivity lifetime measurements.

The fluorescence and phosphorescence lifetime measurements as well as the polarization measurements utilized basically the same apparatus, whereas the photoconductivity experiments utilized a different apparatus. The procedure utilized in each of these measurements was also different. The next sections are therefore devoted to giving a description of the apparatus and procedure used in making the previously mentioned measurements. Also included is a section on sample preparation.

Sample Preparation

The experiments were conducted on sapphire samples obtained from four different companies: Crystal Systems, International Sapphire (Insaco), Linde, and Adolf Meller. All samples were nominally ultraviolet grade, but all showed to a more or less degree the 204 nm F band.

The Linde sample, when received, was irradiated with approximately 10^{18} fast neutrons to introduce the F band. All samples were about 1 mm thick and were polished to an optical finish using diamond paste.

The samples obtained from different companies were grown using one of two different techniques. The Insaco and Linde samples were grown by using the Czochralski growth technique while the Crystal Systems sample was grown by using the Schmid-Viechnichi growth technique, which is an adaptation of the Bridgeman technique.

The Schmid-Viechnichi technique involves directional solidification from a melt. A seed crystal is placed directly over a heat exchanger which uses the flow of helium gas as the heat removal medium. This allows the temperature gradient of the solid throughout its growth to be controlled. The temperature gradient in the liquid is then controlled by the furnace temperature.

The Czochralski growth process involves pulling of a sapphire from a melt of alumina. This requires that the seed and resulting sapphire be rotated while it is pulled. The melt is maintained at a constant temperature by the furnace while a temperature gradient is set up in the solid by the rate the crystal is pulled.

In both techniques growth occurs in a reducing atmosphere either a vacuum or argon gas. Both processes produce sapphire which is of quite high purity. Table II is a listing of impurities and their concentrations that were found to be present in the samples used in the experiments. The impurities and concentrations are thought to be typical of sapphires grown by the forementioned processes.

TABLE II

LIST OF IMPURITIES PRESENT IN Al_2O_3

Impurities	Sample			
	Crystal Systems (ppm)	Insaco (ppm)	Adolf Meller (ppm)	Linde (ppm)
Cr	<10	30	≤50	≤40
Fe	130	100	20	15
Mn	<10	<10	10	25
V	<10	<10	30	20

Fluorescence, Polarization and Phosphorescence Apparatus

The fluorescence experiments were carried out by using the apparatus illustrated in the block diagram shown in Figure 6. The main components were the light source, chopper, lens, filters, shutter, cryostat system, photomultiplier, oscilloscope, and camera.

The light source was a 30/60 watt deuterium lamp which has a large output in the ultraviolet region of the spectrum, especially near 200 nm. The light was mechanically chopped to produce light pulses which had a duration of approximately 10 msec and a rise and fall time of 1 msec. The light pulses were focused through an electronic shutter and an interference filter onto the sample.

The excitation energy was selected by an interference filter, Oriel G-522-2000, with a peak transmission at 200 nm and a band width of 20 nm. The sample was held in a continuous flow cryostat made by Oxford Instruments (CF 204) which was accompanied by an associated digital temperature controller. The sample was placed in the sample container of the cryostat by mounting it on an insert which fits through the top. The chamber containing the sample was evacuated and subsequently filled with helium exchange gas.

Liquid helium is pumped through the GFS 300 transfer tube to the cryostat then back through the transfer tube to the Oxford Instrument digital temperature controller (DTC-2). The temperature displayed by the temperature controller is reported by the manufacturer to be accurate to ± 0.5K of the true sample temperature. The temperature range of the cryostat system is 4.2K to 300.0K.

The light emitted by the sample passed through a Corning glass

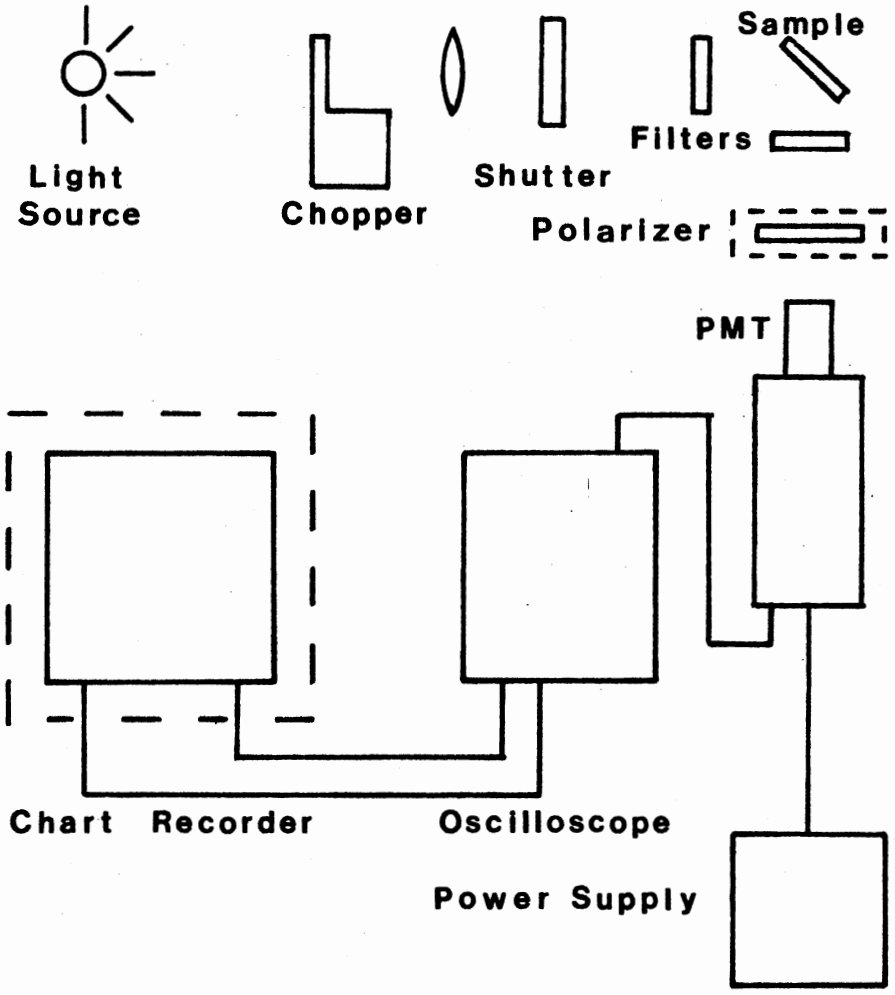

Figure 6. Apparatus for Fluorescence Measurements. The chart recorder was added for the phosphorescence experiments and the polarizer was added for the polarization experiments

filter to an EMI 9813-B photomultiplier tube. The color filter used was either a 0-51 or a 0-52 which has a cutoff wavelength below which less than 1% of the incident light is transmitted, at 361 nm and 345 nm respectively. The resulting signal was amplified and displayed on a Tektronics 7603 wide band oscilloscope, which was equipped with a time base module (7B50A) and an amplifier module (7A16A). The display screen was photographed with a Polaroid camera, from these photographs the data was obtained.

The apparatus used in the polarization experiments is the same as used in the fluorescence experiments except a sheet of polarized material was added.

The polarized material had a known orientation for which it would pass the electric field component of light. In order to check to see if light was polarized it was necessary to be able to rotate the polarized material. This was done by mounting the polarizer on a rotating mount. The polarizer was placed between the color filter and the photomultiplier tube thus allowing for the checking of the polarization of the emission from the crystal.

In the phosphorescence experiments the chopper was removed so that the crystal could be continuously exposed to the exciting light. The signal from the photomultiplier was amplified by the oscilloscope and displayed on the y axis of a Houston Instrument x-y recorder. The x axis of the recorder was driven by the time base generator of the oscilloscope. This allowed the x axis of the recorder to be calibrated to a wide range of time scales.

Photoconductivity Apparatus

Photoconductivity measurements were made near room temperature using an apparatus which has been described in detail previously (12). The apparatus will in this section be described briefly.

The sample holder consisted of a front electrode made of fine, phosphor-bronze wire gauze through which the exciting light could pass. The back electrode consisted of a thin copper foil which was electrically insulated from the cryostat by a thin slab of sapphire.

An electric field was produced between the two electrodes by connecting a battery across them, in this way electric fields of approximately 1000 volt/cm could be established. The direction of these fields could be reversed whenever necessary to permit depolarization of the sample. The field though, was always parallel in direction to the direction of the incident light which was provided by a 30/60 watt deuterium lamp. No filter was used in this experiment so that a maximum signal could be obtained. The light from a deuterium lamp has a maximum near 200 nm which is around the absorption band of the F-center in α-Al_2O_3. The output then falls off rapidly in intensity with increasing energy making the 6.1 eV absorption band the prime candidate for any observed effects. The photocurrent was detected and amplified by a Cary 401 vibrating reed electrometer. The amplified signal was then recorded on an x-t recorder.

The cryostat used did not have any temperature control mechanism so that the sample had to be warmed by blowing air through the cryostat. This allowed the helium exchange gas around the sample and subsequently the sample to warm up to the next temperature value of interest. As the desired temperature was approached the air was turned off and the temper-

ature allowed to stabilize. It was observed that the temperature changed by approximately 1K during a data run.

Fluorescence Procedure

The first step in the fluorescence experiments was to cool the cryostat and sample down to the lowest temperature to be considered. This temperature was then maintained for at least 15 minutes before any measurements were taken. It usually required about 90 minutes to cool the cryostat down to 4K. During this time all electronic equipment was allowed to stabilize.

After the sample had stabilized at the desired temperature the deuterium lamp was turned on and the shutter opened. The crystal orientation with respect to the incoming light was next adjusted along with the photomultiplier tube voltage and the oscilloscope gain until a maximum sample signal without reflected stray light was reached. At this point the oscilloscope was displaying a repetitive signal. A photograph of this was taken for future reference on the chopper's characteristics and is shown in Figure 7.

The actual data considered in this thesis was taken by using the shutter system to allow just one pulse of light to fall on the sample. This caused a rapidly rising signal followed by a decaying signal which with time reached the baseline. A photograph of this single pulse signal was then taken with the oscilloscope on the 10 msec per cm time scale. Since the signal took several hundred milliseconds to reach the baseline the procedure had to be repeated with the oscilloscope on a longer time scale. Also it was necessary to amplify the signal more so that an increased accuracy could be obtained from the photographs as the signal

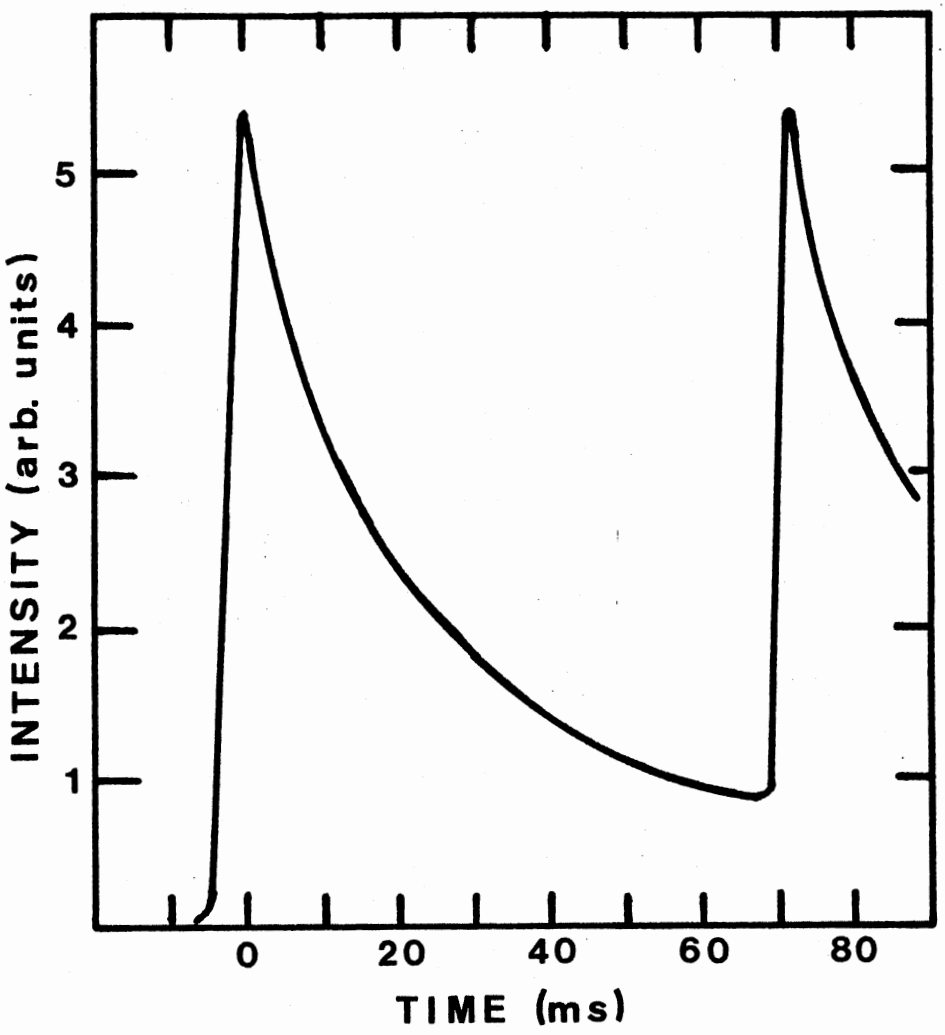

Figure 7. Chopper Characteristics. This is the response of the crystal systems sample to the repetitive signal

approached the baseline. It became necessary to match the data obtained previously with this new data. This was easily done since the zero time position was known in both sets of data. All that had to be done was to normalize the new data so that the magnitudes of both sets of data matched at overlapping time positions. The above procedure was then repeated at approximately 5K temperature intervals up to about 50K. Each time a minimum of five minutes was allowed for the crystal temperature to stabilize. Each time the baseline was checked to insure a minimum of error in interpreting the data.

From 50K to 300K photographs of the single pulse excitation were taken to make certain it agreed with previously reported results. These higher temperature measurements were taken at about 25K intervals.

Polarization Procedure

The C axis of the Adolf Meller sample was found to be in the plane of the crystal. This allowed the C axis to be horizontally oriented on the sample holder as indicated in Figure 8(a). The crystal was then put in the cryostat and oriented so that the angle of incidence of the excitation light was less than a 45° angle with a line perpendicular to the crystal face. This is demonstrated in Figure 8(b). The polarizer was then rotated and the emission of the crystal due to single pulse excitation observed. To insure that reflection off of the crystal face was not the cause of the observed room temperature polarization, a second orientation of the crystal was used. The sample holder was rotated so that the excitation light incident on the crystal made an angle of more than 45° with a line perpendicular to the crystal face. This configuration is shown in Figure 8(c). The signal was then rechecked for polari-

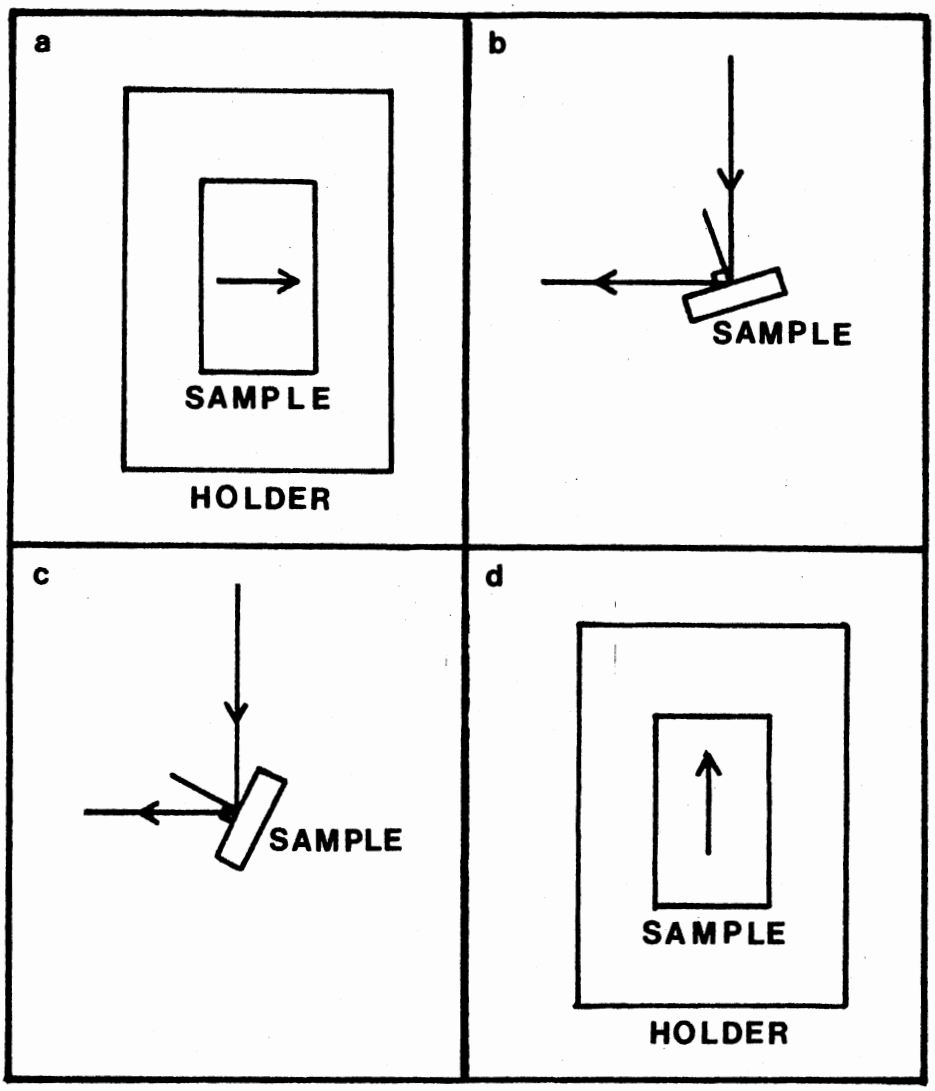

Figure 8. Crystal Orientation for the Polarization Experiments. In a and d the arrow represents the orientation of the crystal's C-axis. The orientation of the sample with respect to the excitation light is demonstrated in b and c

zation.

It was found that the Crystal Systems sample's C axis was in the face of the crystal. The crystal was then mounted on the cryostat insert with it's C axis vertical as indicated in Figure 8(d). The experiment performed on the Adolf Meller sample was then repeated on the Crystal Systems sample.

The single light pulse polarization experiments were repeated from 5K to 300K on the Crystal Systems crystal. The C axis of the crystal was oriented as in Figure 8(d). From 5K to 50K checks on the polarization of the fluorescence emission were done at 5K intervals to 25K then at 10K intervals to 50K. From 50K up the polarization checks were done at random intervals. This experiment was to determine if further experiments were needed. The intensities of the emission were checked with the polarizer set to pass the electric field of the emission perpendicular then parallel to the crystal's C axis. These intensities were then recorded.

The polarization experiments were repeated a second time on the Crystal Systems sample at temperatures of 20K and 50K. At 20K the signal was photographed with no polarizer present, with the polarizer at a setting to get a maximum signal through, and finally with the polarizer set to get a minimum fluorescence signal through. At 50K the fluorescence signal was photographed with just the chopper on to get a repetitive signal. This was done with the polarizer in a maximum and then in a minimum position for maximum and minimum fluorescence signal. Next the shutter was again used to get a single light pulse from the chopper. The resulting signal was photographed with the polarizer in a maximum and a minimum position as described before.

Phosphorescence Procedure

Phosphorescence experiments were performed from about 217K to 300K. For this experiment the light chopper was removed and the x-y recorder connected to the oscilloscope as described in the apparatus section.

The sample temperature was lowered to 271K and allowed to stabilize. Next the proper settings on the x-y recorder and oscilloscope were chosen as well as the proper photomultiplier voltage. The x-y recorder was then started and the shutter opened to the 200 nm excitation light. When the signal reached a maximum the shutter was closed causing the signal to begin to decay to the baseline. This procedure was repeated at 7K intervals from 271K to 300K.

Photoconductivity Procedure

The photoconductivity experiments were conducted over a temperature range of about 264K to 292K in 7K steps. The same deuterium lamp used in the phosphorescence experiments was used in this experiment, although no filter was used to select out any certain excitation energy. It was thought that it would not matter how the electrons were excited into the conduction band. What should matter is what happens after the excitation light is shut off.

The data was taken with the applied electric field in the same direction as the incoming photons. It was necessary after each exposure of the crystal to the excitation light to depolarize it. This was accomplished by reversing the direction of the electric field and then exposing the crystal to the excitation photons.

The amplified photoconductivity signal was recorded on an x-y recorder equipped with a time base module to drive the horizontal axis. In this way a plot of the photoconductivity signal voltage against time was obtained. After the plot was obtained the sample was depolarized and the temperature increased to the value for the next reading.

CHAPTER III

RESULTS

Introduction

The fluorescence experiments were conducted in detail on two samples of sapphire. These were the Crystal Systems and Insaco samples. Photographs of the fluorescence signal from the neutron irradiated Linde sample were taken and analyzed but were more difficult to interpret due to the weakness of the signal. The reason for this weakness seems to be due to concentration quenching. It was however possible to determine that the measurements to be discussed later for the Crystal Systems and Insaco samples were also confirmed for the Linde sample. The Adolf Meller sample was checked visually and found to also exhibit similar properties to those of the Crystal Systems and Insaco samples. It was also found that all the samples showed similar emission bands, this is discussed next.

Luminescence Spectrum

As a preliminary investigation the luminescence spectrum excited by 6.2 eV light was observed. The data presented here was recorded and analyzed by G. P. Summers (13) and is summarized here at his suggestion. The luminescence spectrum for the Crystal Systems sample is shown in Figure 9 at several different temperatures. The vertical scales in this figure have been shifted relative to one another to avoid overlap

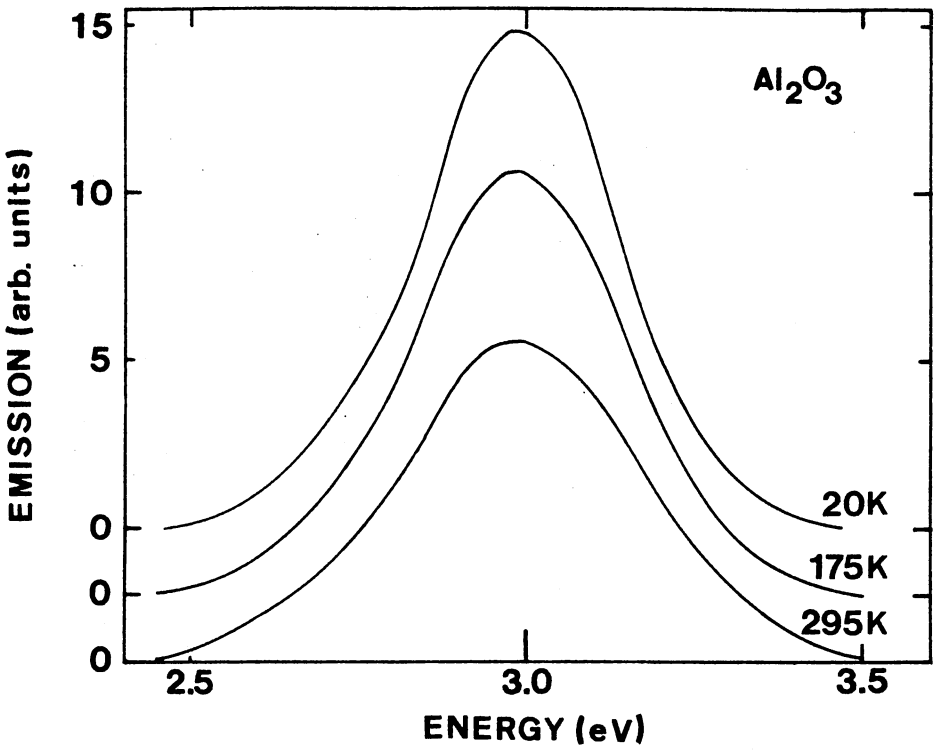

Source: G. P. Summers (13)

Figure 9. Luminescence Spectrum

of the spectra. Similar spectra were obtained from each of the other samples. Inspection of these spectra indicates that the peak position at 3.0 eV is almost independent of temperature over the range of 20K to 300K and that the full width at half maximum intensity is noticeably temperature dependent above 100K. In addition the spectral dependence of the band is almost Gaussian, although at the lowest temperatures a slight low energy tail becomes apparent.

The conclusion drawn from the luminescence spectra is that if the sample is excited in the F-center absorption band (6.1 eV) then the emission band is centered about the 3.0 eV F-center emission band. Further the emission has no other bands. This indicates that the fluorescence emission to be considered in the next section is due only to this 3.0 eV emission band. With this established the F-center fluorescence emission can be discussed.

Fluorescence Results

The data from the single pulse excitation fluorescence experiments proved to be most interesting. In Figure 10 is a logarithmic replot of an actual photograph taken of the fluorescence emission for the Insaco sample at about 4K. It is obvious from this that the decay is composed of more than one exponential decay. It becomes even more clear when the data is plotted along with a fit to a function composed of two exponential decaying terms plus a constant such as is done in Figure 11 where the dots are the data points and the line is the fit obtained from the function. The semilogarithmic plot makes it clear that the decay is not a second order process, but to make sure fitting the data to a second order process was tried with no success. It was then determined

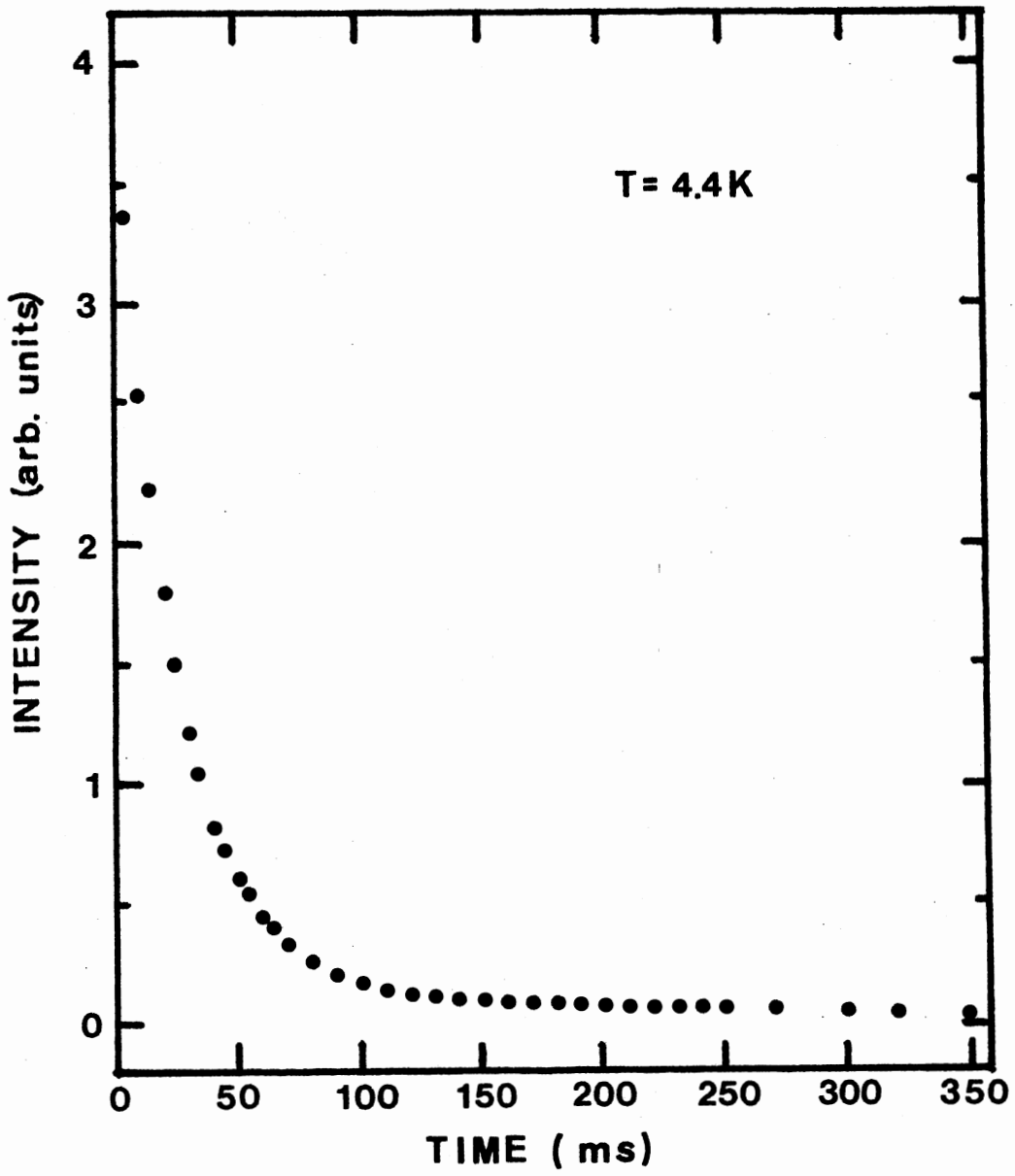

Figure 10. Fluorescence Emission at 4K for the Insaco Sample

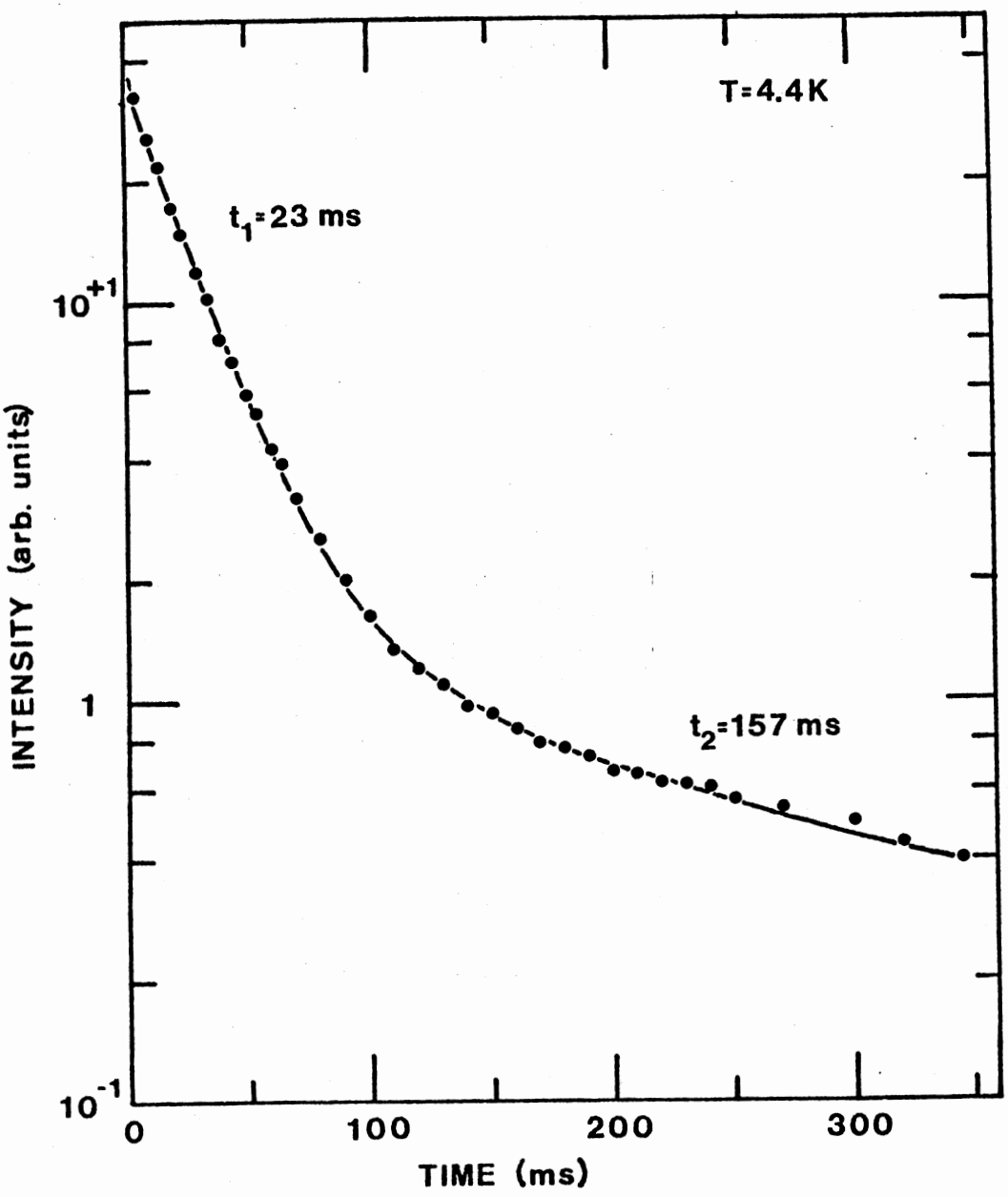

Figure 11. Semilogarithmic Plot of the Fluorescence Emission at 4K for the Insaco Sample

that the data was best fit by using the sum of first order decays, the function being:

$$I = A*EXP(-t/t_1) + B*EXP(-t/t_2) + C$$

where I is the measured intensity of the emission,

A and B are the intensities in the two lifetime components,

t_1 and t_2 are the lifetimes of the two components,

C is a constant.

The constant C is used to compensate for other decay processes which were extremely long compared to the ones being discussed here and also for any baseline error. It is seen from Figure 11 that this function gives an excellent fit.

A summary of the lifetimes and their intensities over a temperature range of 5K to 55K for both the Crystal Systems and the Insaco samples is given in Table III. The error bounds of the lifetimes are thought to be 10% of the lifetime values. The data for the Insaco sample is shown replotted on semilogarithmic graph paper in Figures 12 and 13 for several different temperatures. As previously indicated the dots are the data points and the continuous line is the fit obtained by the use of the first order decays, the lifetimes are also indicated. It is seen that with temperature the actual shape of the fluorescence decay changes. This indicates that the processes involved are temperature dependent. This is clearly reflected in the lifetimes and their intensities obtained from the fits. The fits shown in the figures are seen to be quite good which allows the fitting parameters to be used for interpreting the data. Equally good fits were also obtained to the Crystal Systems emission data.

TABLE III

LIFETIME DATA FOR FLUORESCENCE

Temperature (K)	A (Arb. Units)	t_1 (msec)	B (Arb. Units)	t_2 (msec)	C (Arb. Units)
Insaco:					
4.4	3.77	23.4	0.179	157	0.0192
10.4	4.77	23.2	0.213	168	0.0209
15.6	4.75	23.5	0.238	157	0.0185
20.4	3.93	22.7	0.240	137	0.0150
25.5	3.91	22.7	0.301	131	0.00523
30.5	3.31	20.4	0.868	75.9	0.00423
35.5	1.86	14.4	2.33	47.1	0.00387
40.4	0.94	5.99	3.47	38.1	0.00680
45.5	0.482	3.56	3.76	36.0	0.00753
50.4	0.225	2.04	3.80	34.7	0.00863
Crystal Systems:					
5.0	3.38	24.5	0.179	347	0.0
10.4	3.39	24.7	0.123	441	0.0
15.5	3.43	24.0	0.143	431	0.0
20.3#	4.08	24.2	0.129	264	0.0
25.5	3.93	23.4	0.251	167	0.0
30.4	3.35	20.0	0.825	80.4	0.00301
35.5	1.85	15.2	2.17	49.1	0.00148
40.4	0.744	7.83	3.35	39.7	0.00560
45.4	0.294	3.02	3.61	36.6	0.00821
50.5	0.0	*.*	3.75	35.7	0.00806
55.4	0.0	*.*	3.77	35.4	0.00684

#Data for 20.3K to 55.4K taken from a previous experiment.

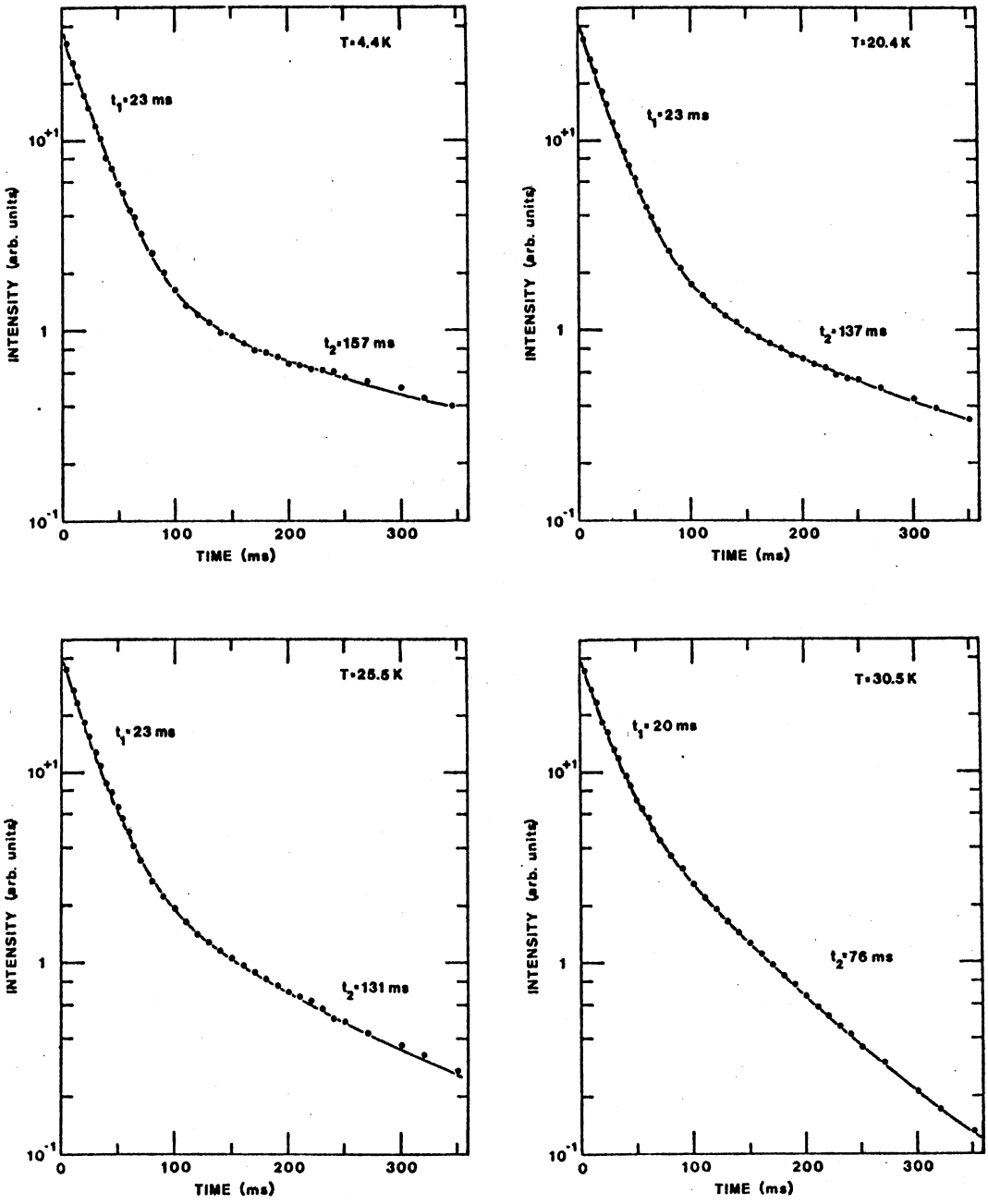

Figure 12. Semilogarithmic Plot of the Fluorescence Emission at Various Temperatures. The lifetimes are indicated by t_1 and t_2. The data is for the Insaco sample

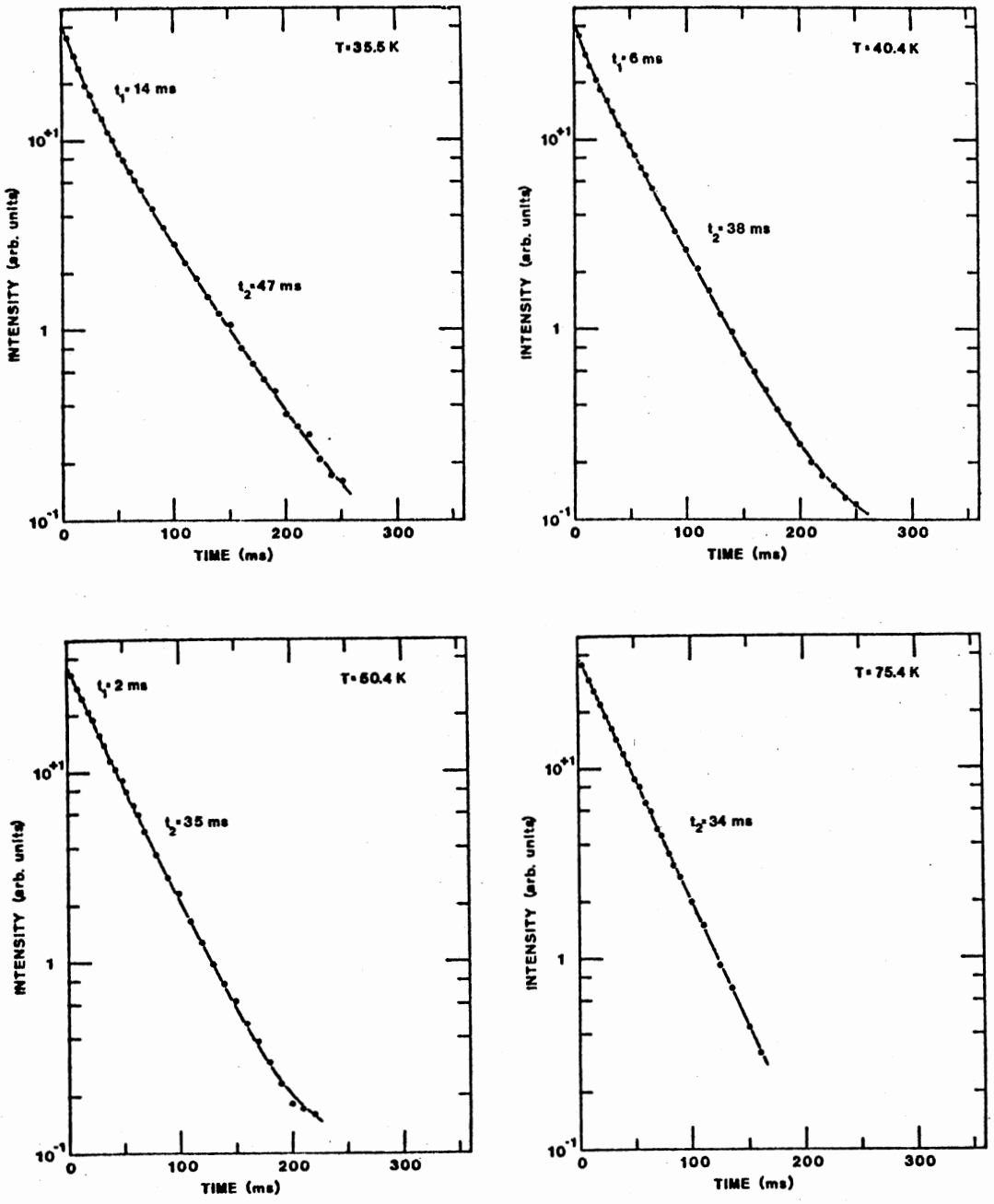

Figure 13. Semilogarithmic Plot of the Fluorescence Emission at Various Temperatures. The lifetimes are indicated by t_1 and t_2. The data is for the Insaco sample

Analysis of the fitting parameters for the Crystal Systems and Insaco emission data indicates that not only were two lifetimes detected at temperatures below 50K but these lifetimes were also temperature dependent. Figure 14 is a plot of lifetime versus temperature for the Insaco sample. A similar temperature dependence was found for the lifetimes obtained for the Crystal Systems data.

It is clear from the data in Table III that the slower lifetime component in the Crystal Systems sample goes from 350 msec to 35 msec over a temperature range of 5K to 45K. The slower lifetime component in the Insaco sample goes from approximately 150 msec at about 4K to approximately 35 msec at 50K. The trend in the 23 msec lifetime is for it to get faster in both samples. From 5K to about 20K the lifetime is constant at about 23 msec, then at around 30K it begins to get faster until at 50K it is practically gone or at least too fast for the equipment used to measure it.

The relative intensity in each lifetime component can be found by multiplying the lifetime and the intensity of the component at t = 0 together. The relative intensities are given in Table IV for the Insaco and Crystal Systems samples. A plot of the relative intensity versus temperature is shown in Figure 15 for the Insaco sample.

At the same time that the lifetimes are growing faster the relative intensities also are changing. The relative intensity of the fast component (t_1 = 23 msec at 4K) rises to a peak at about 15K in the Insaco sample then decreases to near zero at 50K. It is not certain at this point whether the peak is a real effect due to an alignment problem in the apparatus or an effect due to errors inherent in the analysis.

The relative intensity of the long lived component (t_2 = 180 msec

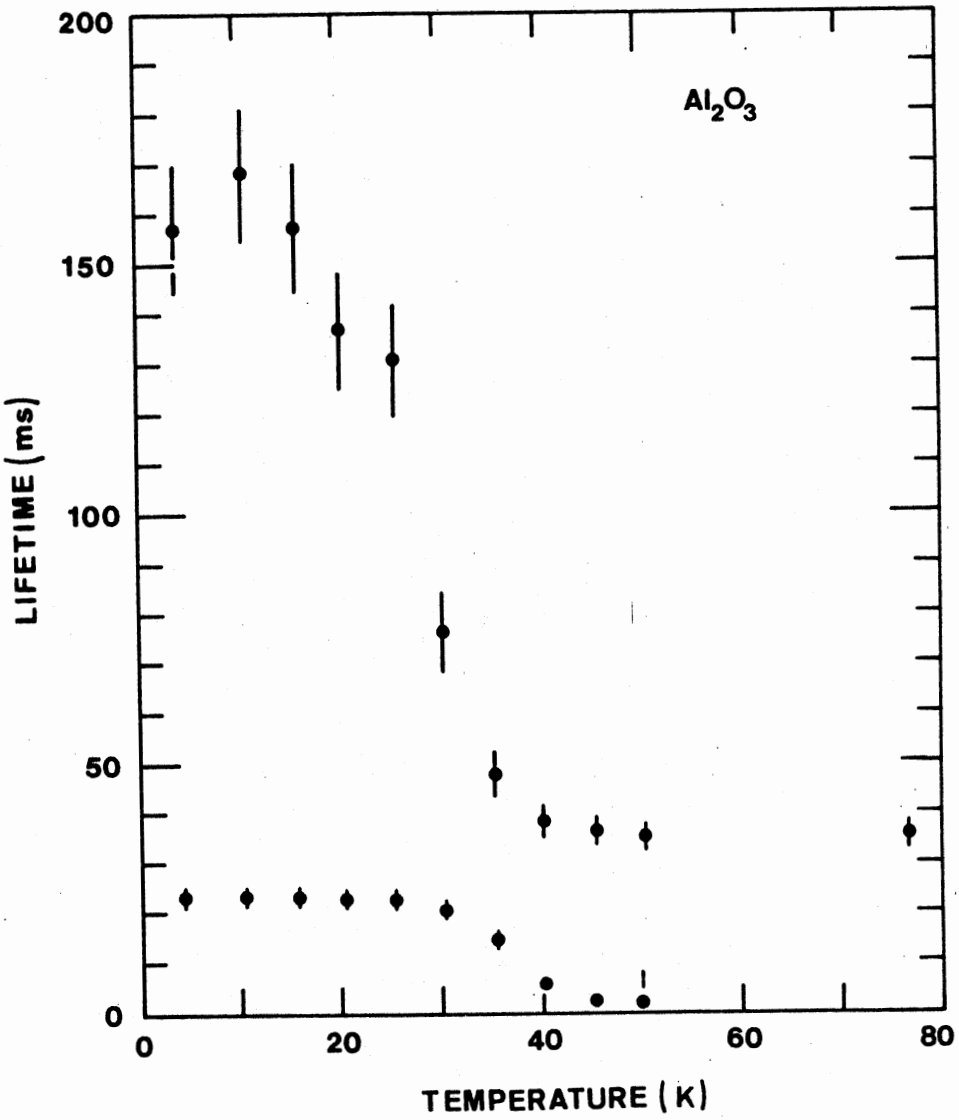

Figure 14. Plot of Fluorescence Emission Lifetime Versus Temperature for the Insaco Sample

TABLE IV

RELATIVE INTENSITIES FOR FLUORESCENCE DATA

Temperature (K)	Axt_1	Bxt_2	$Axt_1 + Bxt_2$	C	$Axt_1 + Bxt_2 + C$
Insaco:					
4.4	0.0882	0.0281	0.1163	0.0192	0.1355
10.4	0.1107	0.0358	0.1465	0.0209	0.1674
15.6	0.1116	0.0374	0.1490	0.0185	0.1675
20.4	0.0892	0.0329	0.1221	0.0150	0.1371
25.5	0.0888	0.0394	0.1282	0.00523	0.1334
30.5	0.0675	0.0659	0.1334	0.00423	0.1376
35.5	0.0268	0.1097	0.1365	0.00387	0.1404
40.4	0.0056	0.1322	0.1378	0.00680	0.1446
45.5	0.0017	0.1354	0.1371	0.00753	0.1447
50.4	0.0005	0.1319	0.1324	0.00863	0.1410
Crystal Systems:					
5.0	0.0829	0.0622	0.1451	0.0	0.1451
10.4	0.0836	0.0543	0.1379	0.0	0.1379
15.5	0.0822	0.0616	0.1438	0.0	0.1438
20.3#	0.0987	0.0341	0.1328	0.0	0.1328
25.5	0.0920	0.0419	0.1339	0.0	0.1339
30.4	0.0670	0.0663	0.1333	0.00301	0.1363
35.5	0.0281	0.1070	0.1351	0.00148	0.1366
40.4	0.0058	0.1330	0.1388	0.00560	0.1444
45.4	0.0009	0.1320	0.1330	0.00821	0.1412
50.4	0.0	0.134	0.134	0.00806	0.1421
55.4	0.0	0.134	0.134	0.00684	0.1408

#Data for 20.3K for 55.4K taken from a previous experiment.

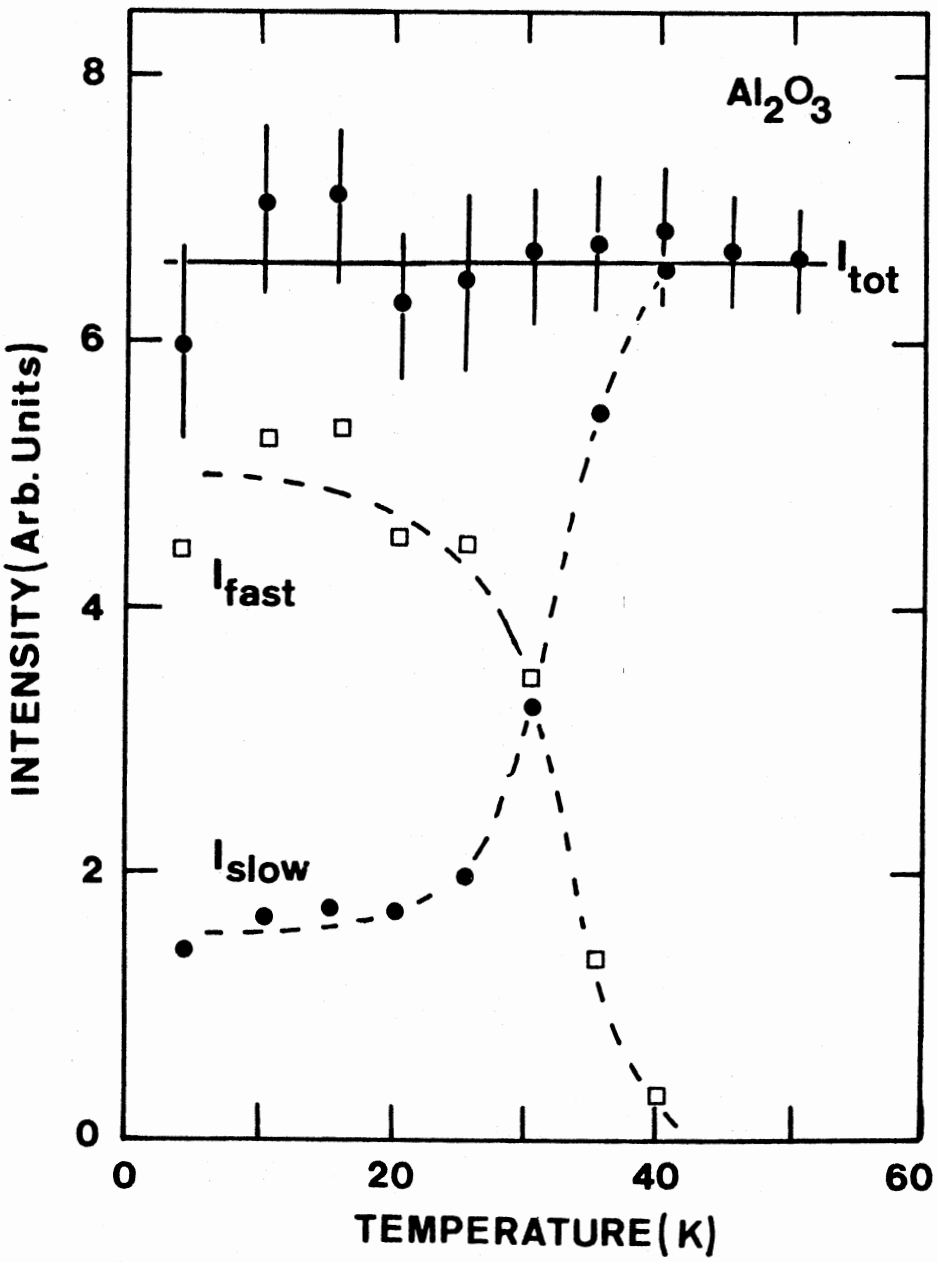

Figure 15. Plot of Relative Intensity Versus Temperature for the Insaco Sample

at 4K in Insaco) starts off approximately as a straight line, then at about 25K it starts to grow. At approximately 40K this component stops growing and levels off, now having almost all of the relative intensity.

For temperatures above 50K the fluorescence lifetime was found to have no temperature dependence. The data was easily fit to a single first order process which yielded a lifetime of 35 msec ± 3 mesc. This value is in good agreement with other reported values.

In summary it is found that, unlike the single first order decay reported for temperatures above 70K, two first order temperature dependent decays are present at temperatures below 50K. One lifetime has a value of 23 msec ± 2 msec at temperatures below 25K and the other lifetime has an order of magnitude of 200 msec below 25K. The actual value of the 200 msec lifetime appears to be sample dependent. At temperatures below 25K most of the relative intensity is in the 23 msec component. As the temperature increases the lifetime and relative intensity of the 23 msec component decrease while the lifetime of the 200 msec component decreases and its relative intensity increases. At 50K the 23 msec component is no longer present and the 200 msec lifetime has decreased to 35 msec ± 3 msec with all of the relative intensity. From 50K to 300K the 35 msec lifetime is the only observable lifetime in the F-center fluorescence emission (3.0 eV emission).

Polarization Checks

Polarization checks of the 3.0 eV fluorescence emission were conducted in detail on the Crystal Systems sample. Room temperature checks were done on the Adolf Meller and Crystal Systems sample to check for possible sources of error.

The experiments previously described in Chapter II are believed to present enough information as to rule out polarization effects due to reflections and any other odd effects. The fact that the signal was substantially polarized whether the crystal face was towards the photomultiplier tube or towards the excitation light should rule out reflection effects. Further the 200 nm interference filter allowed only a narrow range of excitation light to strike the crystal and be possibly reflected. But this possible reflection would still be 200 nm which is well separated from the 360 nm or above which is transmitted by the color filter used to select out the emission wavelength of the F-center. The polarization was also checked with the C axis of the crystal at two different orientations. In each case the polarization was found to be perpendicular to the C axis. This indicates that the polarization was not due to geometric effects.

With the polarization established as being a real effect of the crystal it was decided to investigate the effect at low temperatures. For this the Crystal Systems sample was chosen due to its large fluorescence signal from 5K to 50K.

The maximum signal was found when the polarizer was oriented as to pass an electric field perpendicular to the C axis. The minimum signal was found when the polarizer was oriented as to pass an electric field parallel to the C axis. The ratio of the fluorescence signal strength at maximum and minimum was found to be independent of the temperature.

A separate experiment was later performed on the Crystal Systems sample to determine if the lifetimes previously reported for the F-center fluorescence emission were polarized in the same way. The results are summarized in Table V. The parameters were found by fitting the fluores-

TABLE V

POLARIZATION RESULTS

Temperature (K)	Polarizer Orientation	A (Arb. Units)	t_1 (msec)	B (Arb. Units)	t_2 (msec)	A/B	Axt_1/Bxt_2
20	Not in System	7.39	24	0.355	290	20.8	1.72
	$\perp$ *	4.27	25	0.209	290	20.4	1.76
	$\parallel$ **	3.22	24	0.159	320	20.3	1.52
50	$\perp$	3.56	37				
	$\parallel$	2.80	38				

*Polarizer passes an electric field perpendicular to the C-axis.

**Polarizer passes an electric field parallel to the C-axis.

cence signal intensity to:

$$I = A*EXP(-t/t_1) + B*EXP(-t/t_2) + C$$

where the parameters are the same as used to fit the fluorescence data. The error bound is thought to be 10% of the lifetime value. It is seen that both lifetime components have their electric fields oriented perpendicular to the C axis in all cases.

It is concluded from the results that the orientation of the polarizer has no effect on the lifetimes. Both the 25 msec ± 3 msec and the 290 msec ± 30 msec lifetimes are associated with an emission polarized perpendicular to the C axis of the crystal. The 37 msec ± 4 msec lifetime for temperatures above 50K was also found to have a polarization perpendicular to the crystal's C axis.

Phosphorescence

At temperatures approaching room temperature it was observed that the sample of Al_2O_3 obtained from the Insaco company showed a long-lived phosphorescence.

The data from the phosphorescence experiment was replotted on semi-logarithmic paper with the signal intensity plotted on the vertical logarithmic scale and time plotted on the horizontal scale. Examples of these plots are presented in Figures 16 and 17 for various temperatures. The dots are the data and the line is the fit to:

$$I = I_o \, EXP(-t/t_1)$$

where: I is the signal intensity

I_o is the signal intensity at t = 0

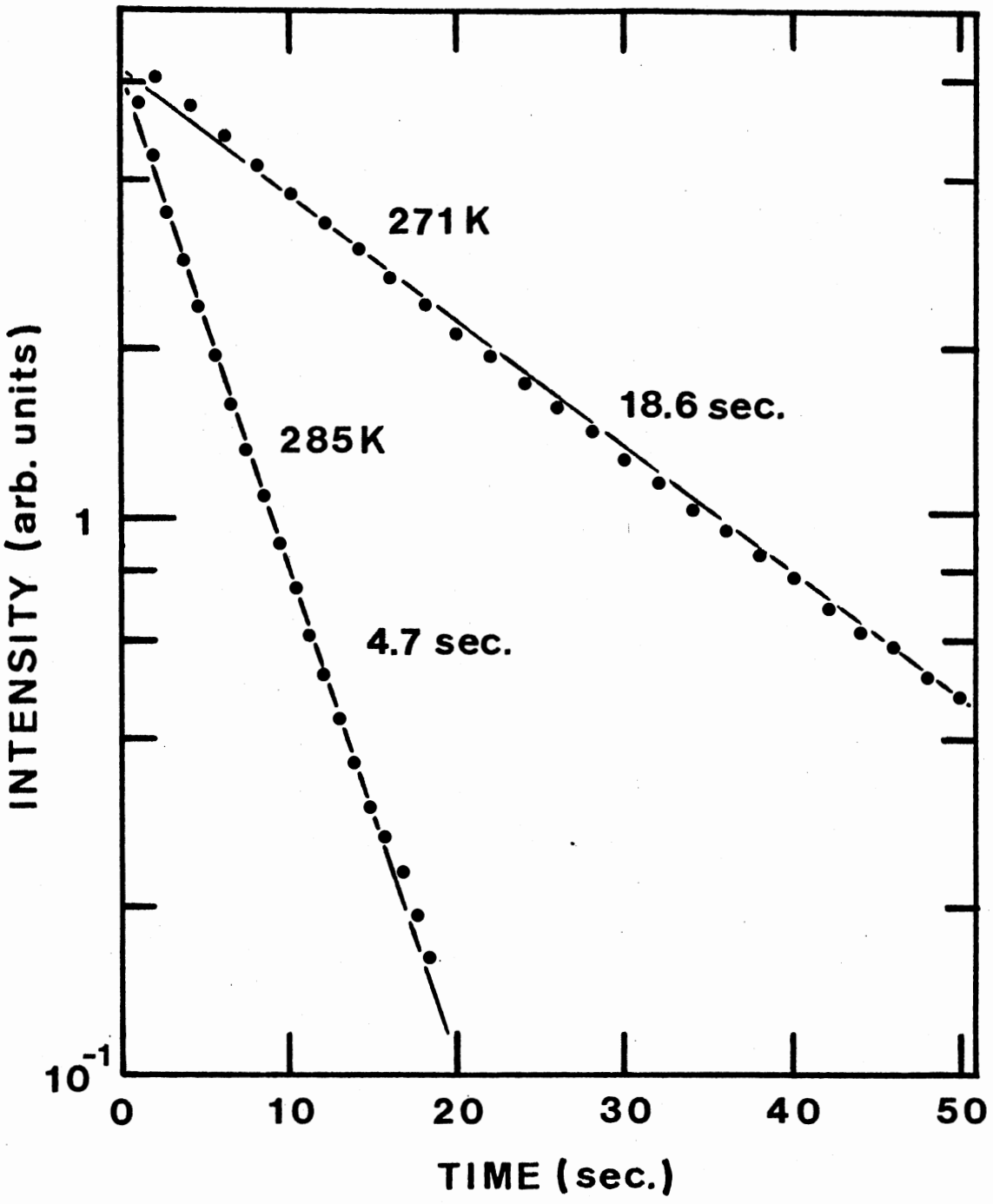

Figure 16. Semilogarithmic Plot of the Phosphorescence Emission at Various Temperatures for the Insaco Sample

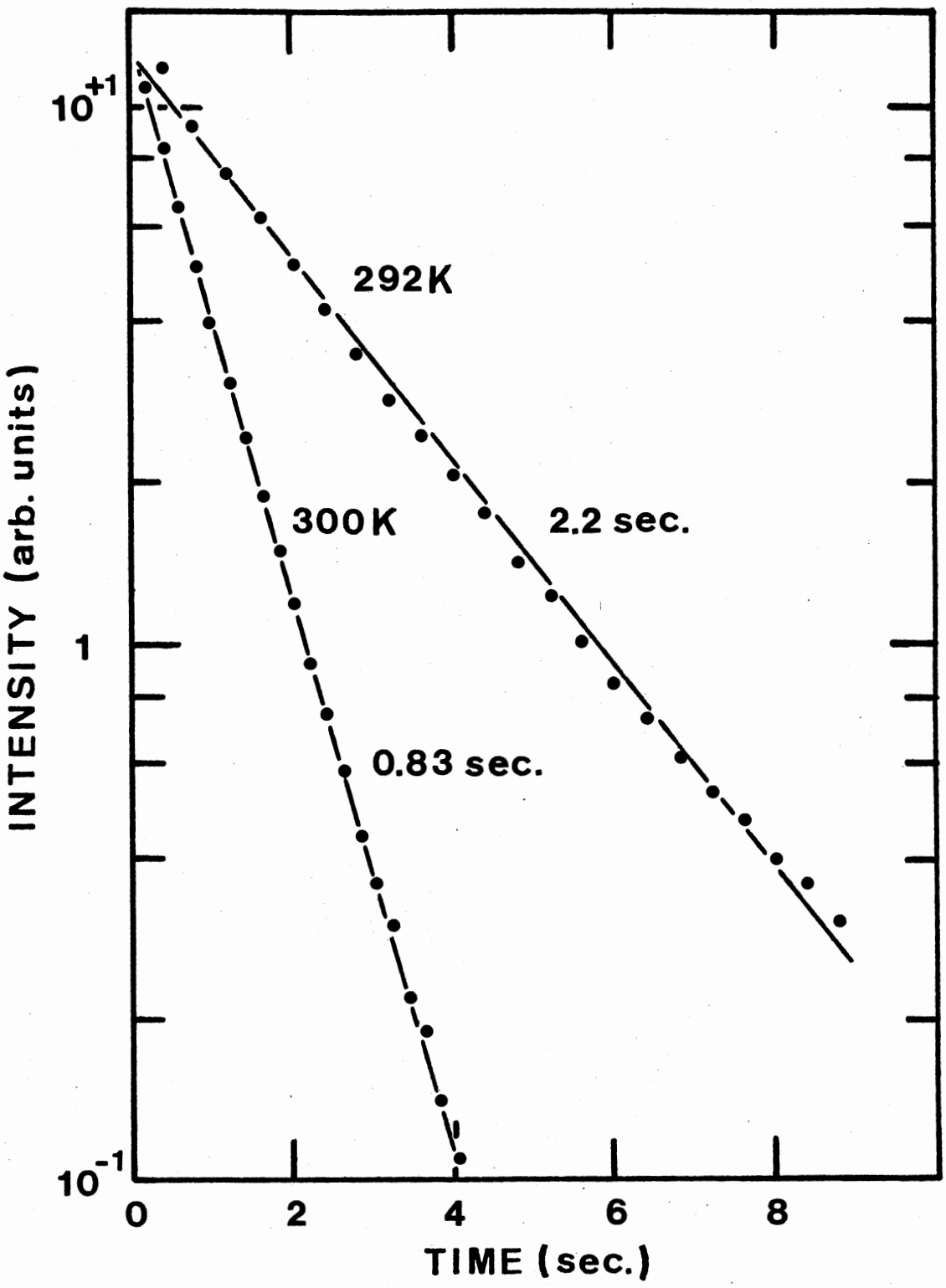

Figure 17. Semilogarithmic Plot of the Phosphorescence Emission at Various Temperatures for the Insaco Sample

t is time

t_1 is the lifetime.

The lifetimes are listed in Table VI.

Photoconductivity Results

In order to better understand the nature of the phosphorescence of the Insaco sample, photoconductivity experiments were later carried out on the same Insaco sample.

The data from the experiment was in the form of a graph of signal intensity versus time. Data of this type was then replotted on semi-logarithmic graph paper with signal intensity on the logarithmic scale and time on the horizontal scale, examples of this type plot for various temperatures can be found in Figures 18 and 19. The data was fit to:

$$I = I_o \, EXT(-t/t_1) + C$$

The constant C is used to compensate for any baseline error. The remaining parameters are the same as described in the phosphorescence experiment. The lifetimes obtained from this fit are listed in Table VII.

TABLE VI

PHOSPHORESCENCE LIFETIME DATA

Temperature (K)	A (Arb. Units)	t (msec)
271.5	6.16	18.6
278.5	6.15	8.6
285.4	6.04	4.7
292.6	12.5	2.2
300.4	13.0	0.83

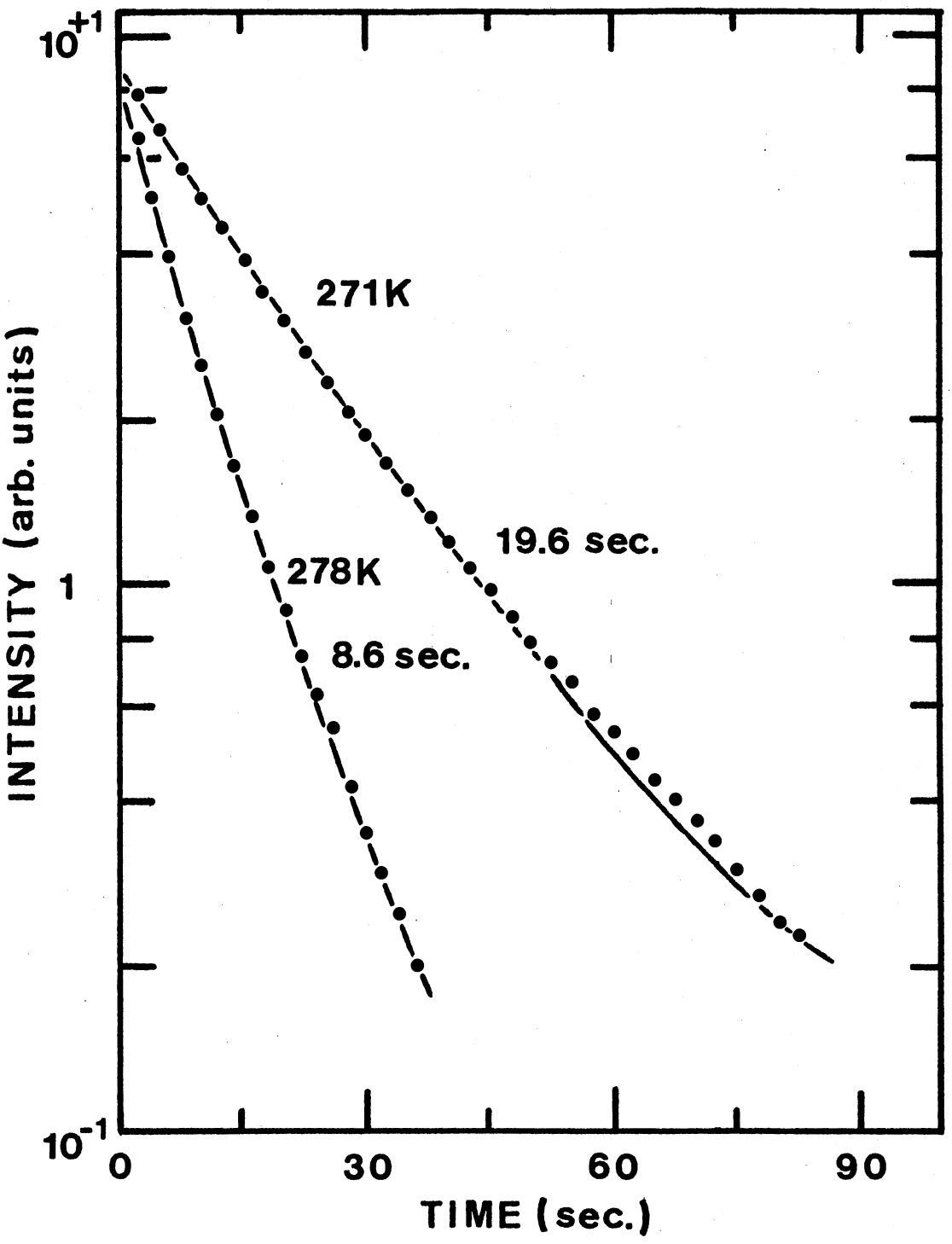

Figure 18. Semilogarithmic Plot of the Photoconductivity at Various Temperatures for the Insaco Sample

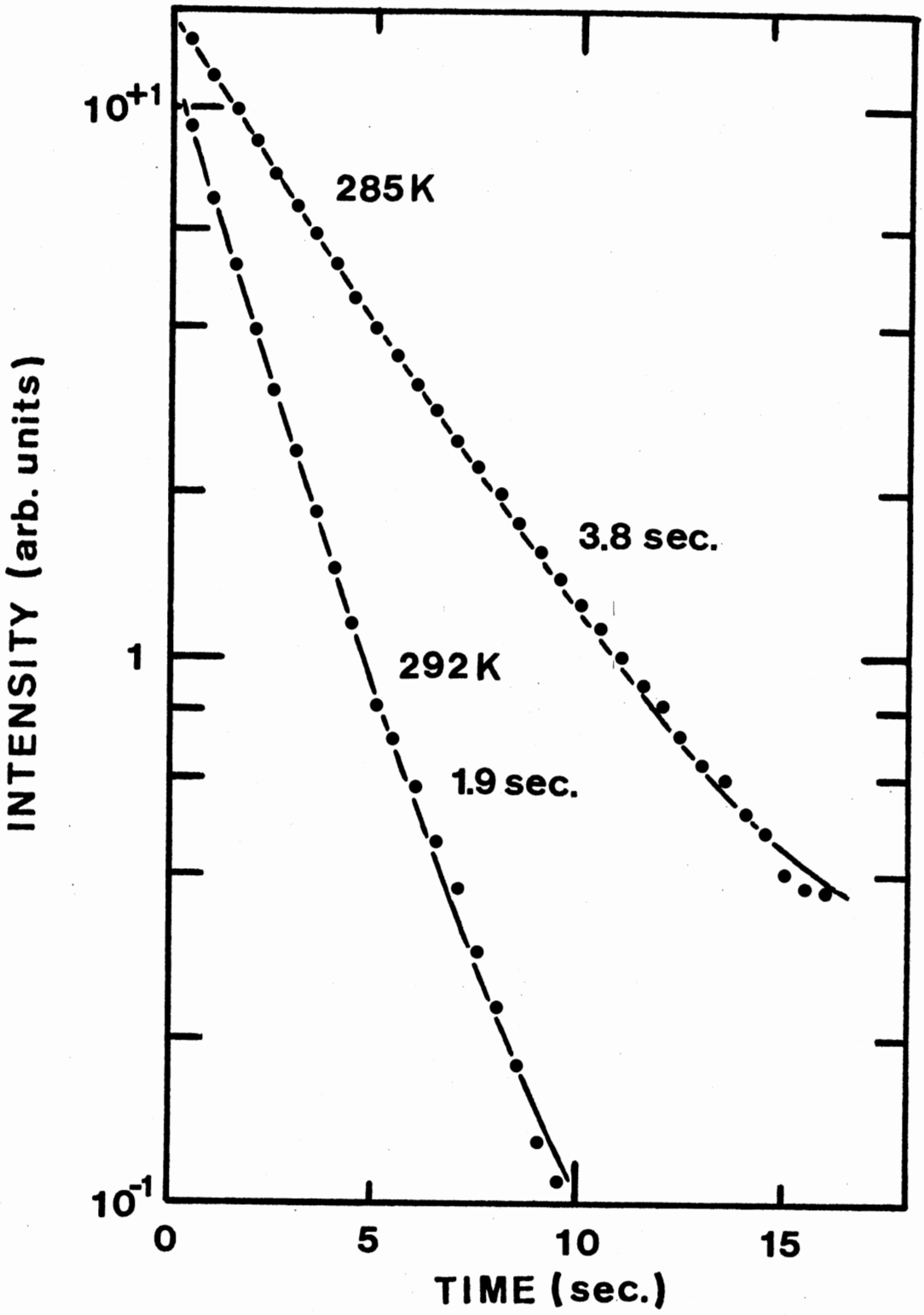

Figure 19. Semilogarithmic Plot of the Photoconductivity at Various Temperatures for the Insaco Sample

TABLE VII

PHOTOCONDUCTIVITY LIFETIME DATA

Temperature (K)	A (Arb. Units)	t (msec)	C (Arb. Units)
263	4.17	38.3	0.07
271	7.37	19.6	0.103
278	6.28	8.57	0.107
285	10.28	3.81	0.163
292	8.90	1.88	0.051

CHAPTER IV

DISCUSSION

Introduction

The fluorescence data has proved to be quite complicated. This is in contrast to what has previously been reported for temperatures above 77K. The fact that below 50K two temperature dependent lifetimes with temperature dependent intensities exist makes the interpretation and explanation somewhat difficult.

At the moment there is no detailed calculation of the electronic structure of the F-center in Al_2O_3 with which to compare the experimental results. In this chapter, therefore, only a preliminary discussion of the fluorescence results will be given. It does seem possible, though, to describe the high temperature phosphorescence and photoconductivity data in terms of a single phenomena and this will be done at the end.

Fluorescence

The notable feature of the very low temperature fluorescence results is that there are two components with different lifetimes, one has a lifetime of 23 msec and the other has a lifetime of the order of hundreds of milliseconds. Low temperature measurements by Draeger and Summers (7) indicate that photoconductivity can be induced in growth colored sample using 6.1 eV light even at very low temperatures, so it

appears that the following model may describe quantitatively the main features observed.

The 6.1 eV band results from the excitation of a F-center electron from the $^1A_1$ ground state to a ^{1}p-like excited state which must be in or very close to the conduction band of the host material. The F-center emission, however, occurs at 3.0 eV which indicates a very large "Stokes Shift" for an F-center. However, the long fluorescence lifetime of the F-center (23 msec) indicates that the transition is forbidden and is possibly from a triplet state. As previously noted the C_2 symmetry of the F-center tends to split the p-like excited state into three components of A_1, B_1, and B_2 character. Separate measurements indicate that the 3.0 eV emission is polarized preferentially with the electric vector perpendicular to the C axis of the crystal, i.e., parallel to the C_2 axis of the center, which is consistent with the 3.0 eV emission being, therefore, from a $^3A_1$ to a $^1A_1$ ground state.

From the relative intensities of the long-lived and short-lived components of the 3.0 eV fluorescence it appears that the electron has about a 20% chance of being released into the conduction band and an 80% chance of returning to the ground state directly. The long-lived component is, therefore, tentatively assigned to the 20% of the electrons which are released into the conduction band. These electrons then may be captured by shallow traps and apparently released even at 4K.

A rough estimate for the depth of these traps can be obtained from a logarithmic plot of the long lifetime versus the inverse of the corresponding temperature as is done for the Insaco sample in Figure 20. The estimate for the depth of the trap is obtained by assuming that the line formed by the data points after the lifetime starts decreasing is

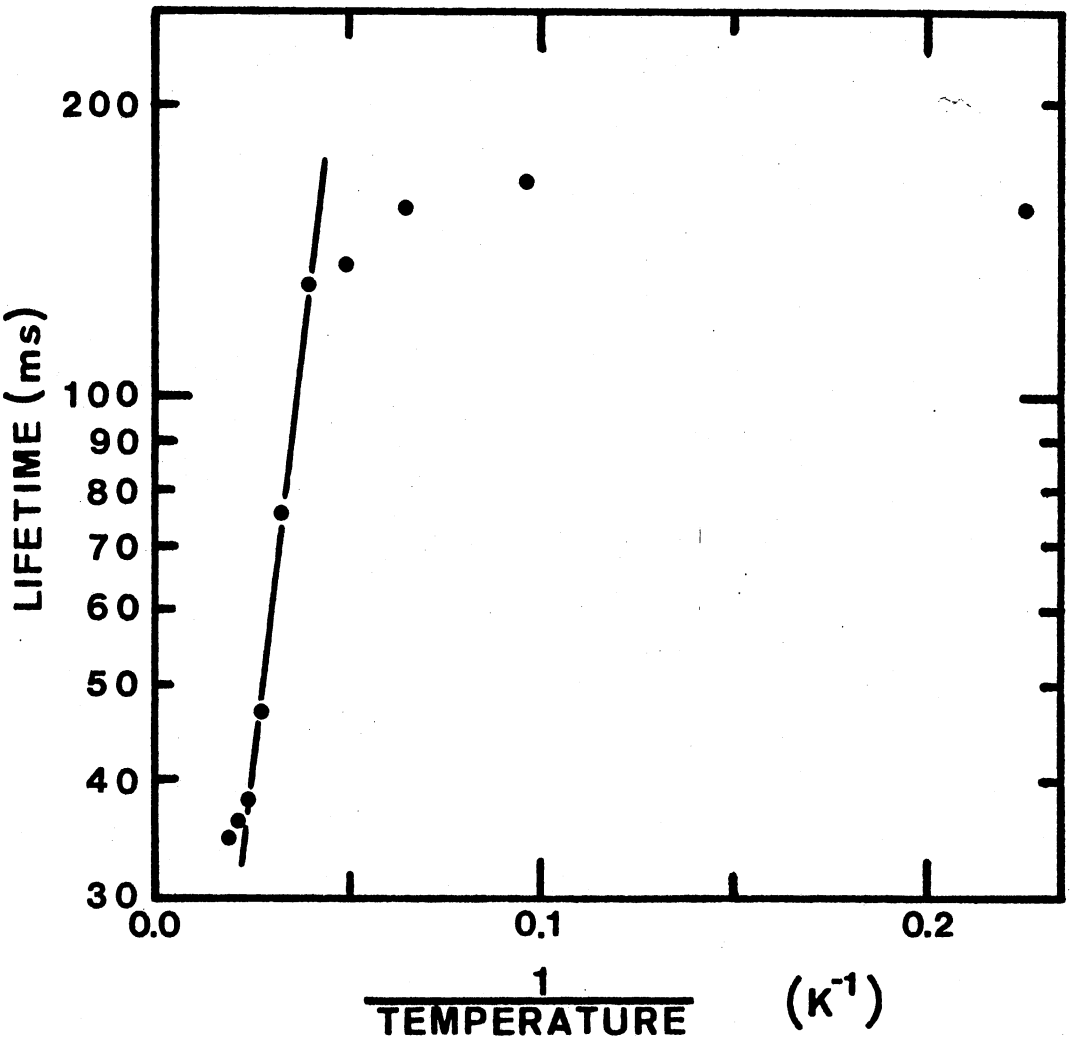

Figure 20. Semilogarithmic Plot of Lifetime Versus the Inverse of the Temperature for the Insaco Fluorescence Emission. The slope of the line gives an estimate of the trap depth

given by:

$$t = t_o \, EXP(E/k_b T)$$

where: t is the lifetime,

t_o is a constant

E is the estimate of the trap depth

k_b is Boltzmann's constant

T is the temperature.

The line formed by the lifetimes then has a slope of E/k_b. The estimate for the trap depth obtained from this method is of the order of magnitude of 10^{-2} eV. The origin of this trap is uncertain but by noting the resemblance in behavior of Al_2O_3 to that of MgO leads to an interesting possibility, the trap might be due to an F^--center as is suggested to occur in MgO.

The fluorescen-e data is then to be interpreted as a long-lived component with its origin due to shallow traps and two other lifetime components, these being a temperature dependent lifetime and a 35 msec temperature independent component. All of these components also have temperature dependent amplitudes. So at temperatures below 30K the emission is dominated by the previously discussed long lifetime and a 23 msec lifetime. At temperatures above 50K both of these components have vanished. Thus for temperatures above 50K the 35 msec lifetime is the only one observed.

What remains to be done is to devise an energy level scheme that will satisfactorily predict the behavior of both the 23 msec and the constant 35 msec lifetime. The energy level scheme that proves to both be simple and yield satisfactory temperature dependence is shown in

Figure 21. In the figure K_1 and K_{12} are nonradiative processes from the conduction band to level 1 and from level 1 to level 2, respectively, K_o is a constant pumping rate from the ground level to the conduction band. The radiative processes k_{10} and k_{20} are transitions from and to the levels as indicated. The population of each level is given by n_0, n_1, n_2 and n_3 for the ground level, level 1, level 2 and level 3 (conduction band), respectively. The rate equations for the energy level scheme are:

$$\frac{d}{dt} n_1 = K_1 n_3 - n_1 (K_{12} + k_{10})$$

$$\frac{d}{dt} n_2 = K_{12} n_1 - k_{20} n_2$$

$$\frac{d}{dt} n_3 = K_0 n_0 - K_1 n_3$$

For the steady state case: $\dot{n}_1 = 0$, $\dot{n}_2 = 0$ and $\dot{n}_3 = 0$. With this condition the populations are given by:

$$n_1 = \frac{K_0}{K_{12} + k_{10}} n_0$$

$$n_2 = \frac{K_{12} K_0}{k_{20} (K_{12} + k_{10})} n_0$$

$$n_3 = \frac{K_0}{K_1} n_0$$

The quantum efficiencies of level 1 (Q_1) and level 2 (Q_2) are given by:

$$Q_1 = \frac{n_1 k_{10}}{n_0 K_0}$$

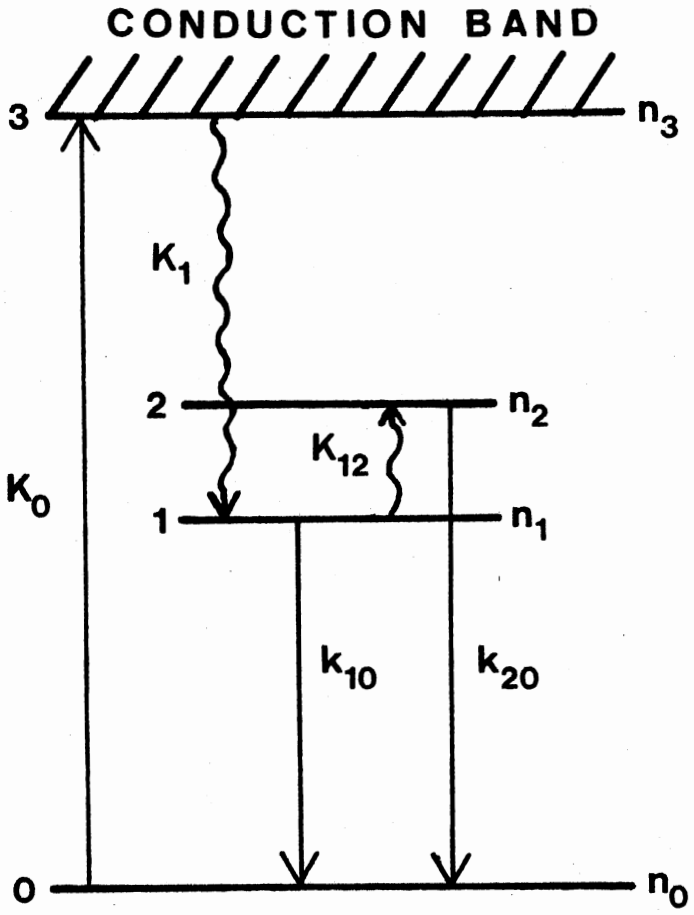

Figure 21. Basic Energy Level Scheme. This represents only part of the proposed energy level scheme for the F-center

$$Q_2 = \frac{n_2 k_{20}}{n_0 K_0}$$

These become:

$$Q_1 = \frac{k_{10}}{K_{12} + k_{10}}$$

$$Q_2 = \frac{K_{12}}{K_{12} + k_{10}}$$

The nonradiative transition 1 to 2 is a thermally activated process so that a form of:

$$K_{12} = K_{12}^{o} \, EXP(-E_{12}/k_b T)$$

can be assumed. K_{12}^{o} is a constant, E_{12} is the energy separation of level 1 and level 2, k_b is Boltzmann's constant and T is the temperature. This expression for K_{12} can now be put in the quantum efficiencies to yield:

$$Q_1 = \frac{1}{1 + B}$$

$$Q_2 = \frac{1}{1 + B^{-1}}$$

where:

$$B = \frac{K_{12}^{o}}{k_{10}} \, EXP(-E_{12}/k_b T)$$

The quantum efficiencies, Q_1 and Q_2, are for steady state conditions but they can also be applied to the non-steady state case such as the fluorescence emission being considered here.

At high temperatures (T greater than 50K) Q_2 must be dominant in order for it to explain the 35 msec lifetime observed in the steady state case as well as the non-steady state case. If K_{12}^{o} is assumed to be on the order of 10^9 sec^{-1}, which is not unreasonable, then it is easily seen that at high temperatures and with the proper choice of E_{12}, say 0.1 eV, that Q_2 approaches one and Q_1 approaches zero. This analysis will be continued after the nonsteady state lifetimes are found.

For the non-steady state, the time after the light source is shut off:

$$\dot{n}_3 = 0$$

A form of:

$$EXP(-wt)$$

where t is time, can be assumed for n_1 and n_2. Putting this substitution into the rate equations yields:

$$-wn_1 = -n_1(K_{12} + k_{10})$$

$$-wn_2 = K_{12}n_1 - k_{20}n_2$$

The w's are given by the zeros of the determinant:

$$\begin{vmatrix} w - K_{12} - k_{10} & 0 \\ K_{12} & w - k_{20} \end{vmatrix} = 0$$

This yields:

$$w_1 = K_{12} + k_{10}$$

$$w_2 = k_{20}$$

Putting in the previously suggested form for K_{12} yields decay rates of the form:

$$w_1 = k_{10} + K^{o}_{12} \, EXP(-E_{12}/k_b T)$$

$$W_2 = k_{20}$$

Where w_1 and w_2 are interpreted as the inverse of the lifetimes for the levels 1 and 2, respectively. In order to better see the temperature dependence of Q_1, Q_2, w_1 and w_2 values for the constants will be assigned as follows:

$$k_{10} = 40 \text{ sec}^{-1}$$

$$k_{20} = 28.6 \text{ sec}^{-1}$$

$$E_{12} = 0.1 \text{ eV}$$

$$\frac{K^{o}_{12}}{k_{10}} = 10^9$$

Plots of Q_1, Q_2, w_1 and w_2 are shown in Figure 22. The plots of Q_1 and Q_2 can be compared with the plots of the relative intensities for the Insaco sample (Figure 15). The plots of w_1 and w_2 can be compared with the plots of lifetime versus temperature for the Insaco sample (Figure 14). From these comparisons it is seen that Q_1, Q_2 and w_1 are of the proper form. If w_2 is associated with a temperature dependent amplitude

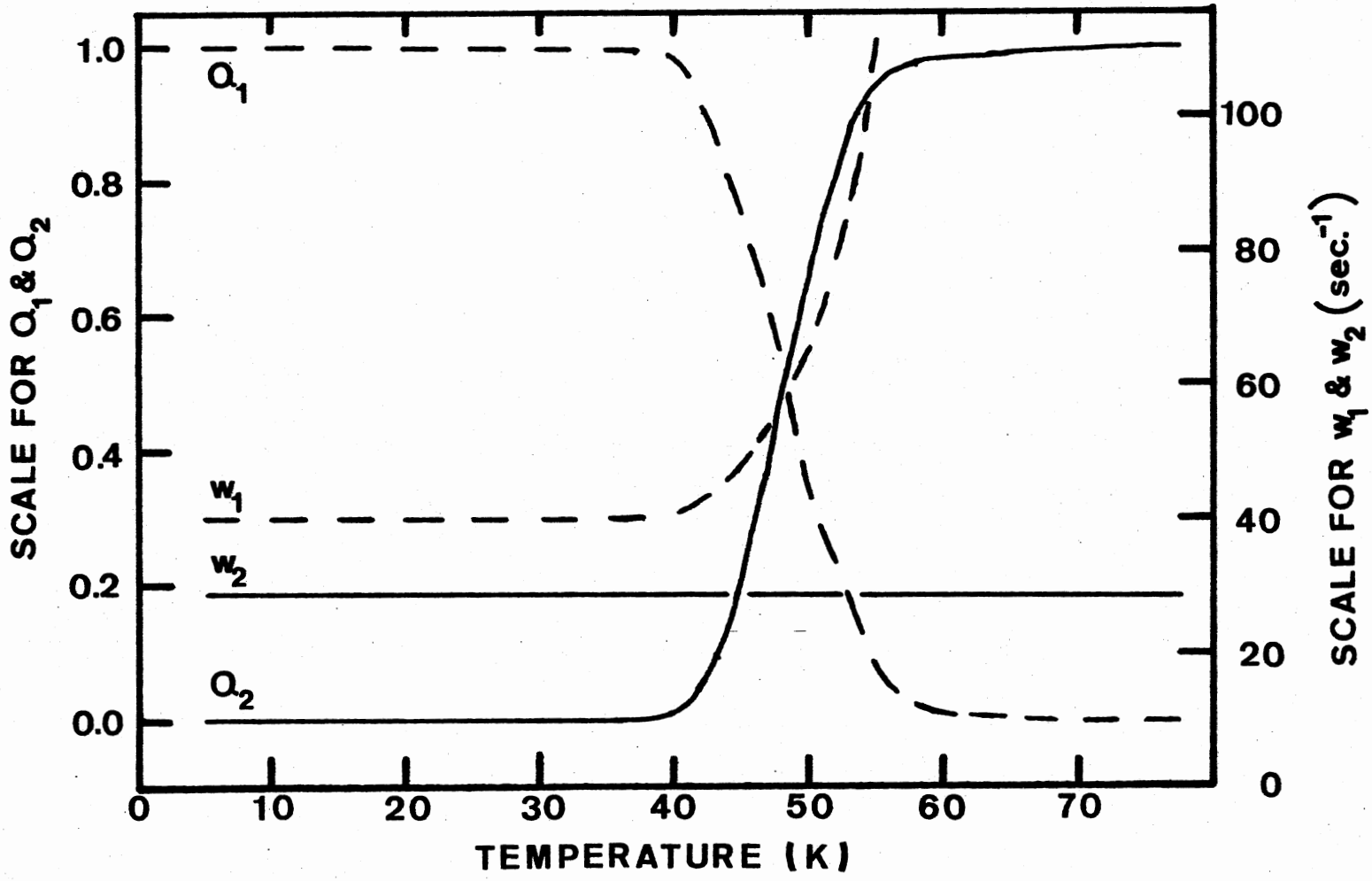

Figure 22. Plots of the Theoretically Determined Lifetimes and Quantum Efficiencies

factor then it too has the correct form. The actual expression for the intensity will next be derived using the same model.

The measured light intensity, normalized to the steady state value, for this system is given by:

$$I = \frac{k_{10}n_1(t) + k_{20}n_2(t)}{K_0 n_0} = f_1 \, EXP(-w_1 t) + f_2 \, EXP(-w_2 t)$$

where: $w_1 = k_{10} + K_{12}^{o} \, EXP(-E_{12}/k_b T)$

$w_2 = k_{20}$

This can be done since the time-dependence of the populations will be a linear combination of components with decay rates w_1 and w_2. In order to evaluate f_1 and f_2 two boundary conditions can be imposed:

1) $I(t=0) = 1$

2) The electrons in levels 1, 2, and 3 must all eventually return to the ground state of the F-center. This implies that

$$\int_0^\infty \frac{dn_0}{dt} \, dt = \int_0^\infty I dt = \frac{n_1 + n_2 + n_3}{K_0 n_0}$$

In the second boundary condition n_1, n_2, and n_3 are the populations of levels 1, 2, and 3 that were found for the steady state case. The second boundary condition can be simplified if the assumption is made that the transition from the conduction band to level 1 is very fast. This implies that:

$$\frac{1}{K_1} << 1$$

i.e.,

$$\frac{n_3}{K_0 n_0} = \frac{1}{K_1} << 1$$

This allows the term in the second boundary condition which contains n_3 to be neglected. The boundary conditions can be expressed as:

1) $f_1 + f_2 = 1$

2) $\frac{f_1}{w_1} + \frac{f_2}{w_2} = \frac{k_{20} + K_{12}}{k_{20}\,(K_{12} + k_{10})}$

From these two equations it is found that f_1 and f_2 are:

$$f_1 = \frac{1}{1 + A}$$

$$f_2 = \frac{1}{1 + A^{-1}}$$

where:

$$A = \frac{K_{12}^{o}}{k_{10} - k_{20}} \mathrm{EXP}(-E_{12}/k_b T)$$

It is seen that f_1 and f_2 have the same basic temperature dependence as the quantum efficiencies Q_1 and Q_2 found earlier. Then f_1 and f_2, as did Q_1 and Q_2, have the proper temperature dependence.

The energy separation of levels 1 and 2 was found by fitting w_1 to the lifetime data of the 23 msec component. It is apparent that:

$$k_{20} = 1/35 \text{ msec}^{-1}$$

$$k_{10} = 1/23 \text{ msec}^{-1}$$

The fit of w_1 to the low temperature 23 msec lifetime data is shown in Figure 23, where the dots are data and the line is the fit. The energy separation of level 1 and 2 is found to be 0.029 eV ± 0.002 eV if the Insaco data is used and 0.032 ± 0.002 eV if the Crystal Systems data is used. K_{12}^0 was found to be 4.4 x 10^6 sec^{-1} for the Insaco data and 8.9 x 10^6 sec^{-1} for the Crystal Systems data. The values for the energy separation, E_{12}, are in excellent agreement for the two samples.

The energy level scheme with the energy separation of the levels, lifetimes and level designations is shown in Figure 24. This model, as has been demonstrated, adequately describes the fluorescence results. It is seen that the shallow trap provides the source for the temperature dependence of the long-lived first order lifetime component when it is assumed that the trap feeds the level associated with the 35 msec lifetime. In this way the 35 msec lifetime component which is present for temperatures above 50K, can have temperature dependence added in at lower temperatures thus explaining how the long-lived component can quicken into the 35 msec lifetime component. The amplitude associated with the 35 msec lifetime is also modified by the trap. As was started the trap can be emptied even at 4K so that by 50K the temperature dependence it adds to the 35 msec lifetime component can vanish. This allows the 35 msec component to be temperature independent above 50K. As demonstrated the temperature dependence of the 23 msec component is easily explained by this model. This F-center model then is one way that the complex temperature dependence of the fluorescence emission (3.0 eV) can be explained.

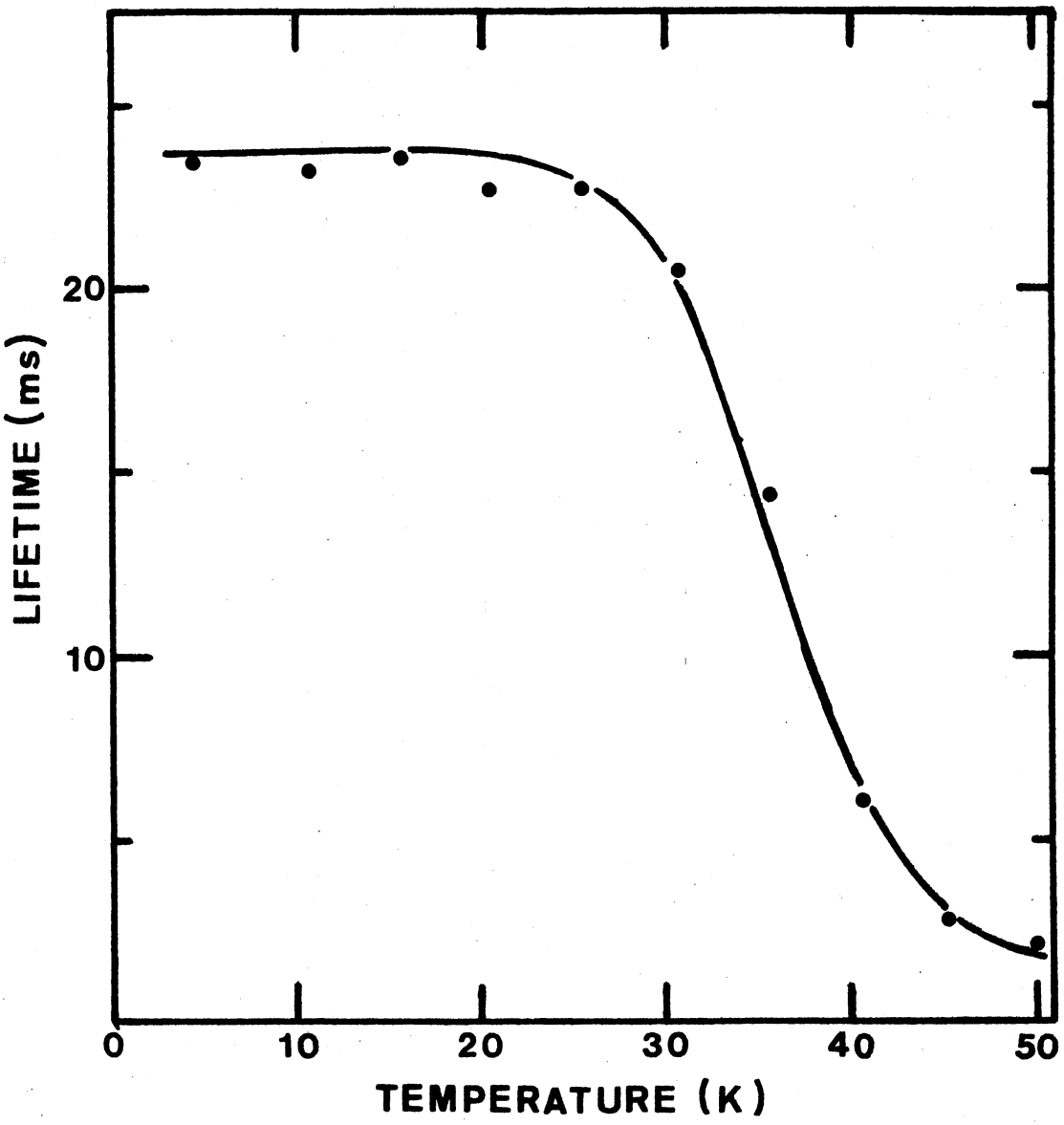

Figure 23. Plot of Lifetime Versus Temperature With a Theoretical Fit. From the fit of W_1 to the fast lifetime component found in the Insaco sample, the energy separation of level 1 and 2 is found to be 0.029 eV

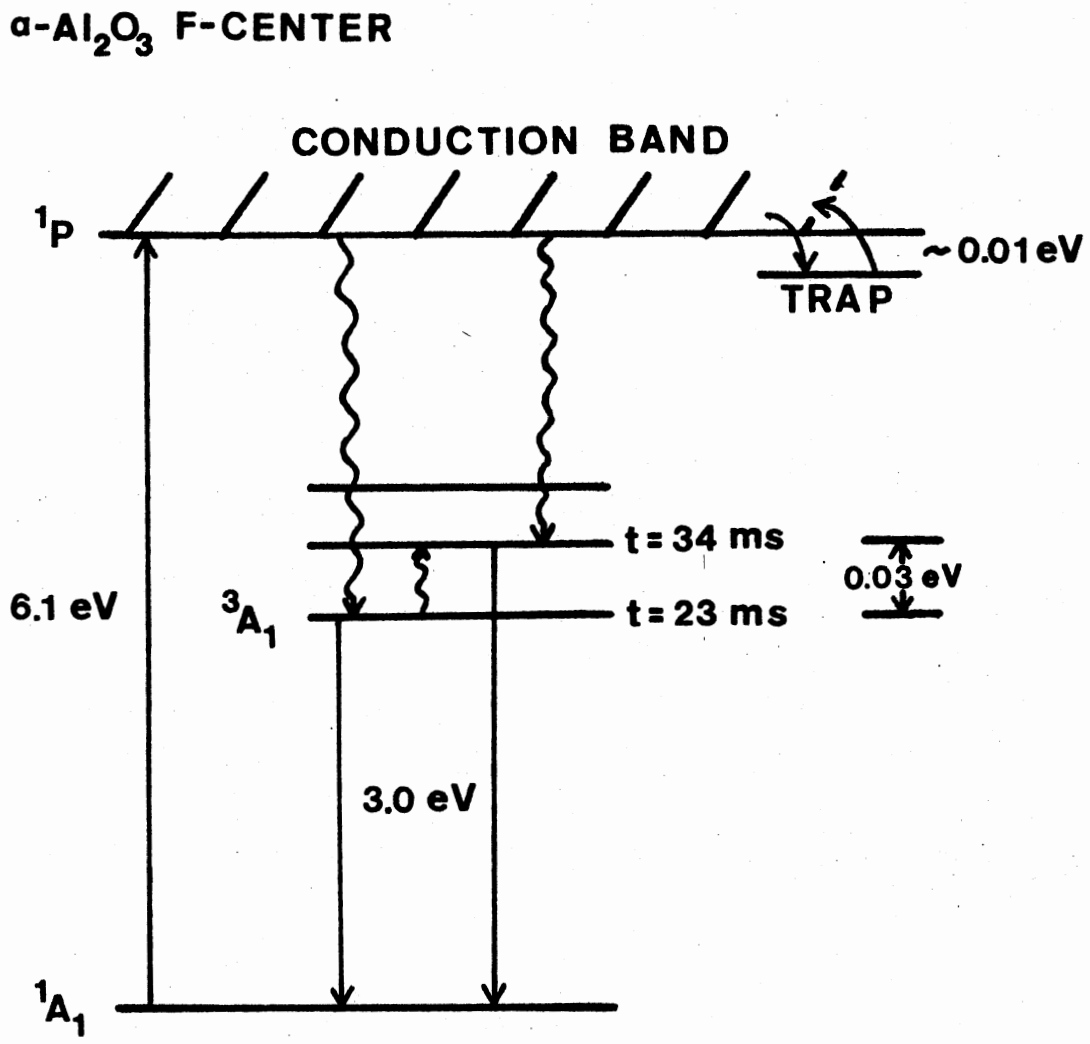

Figure 24. Proposed Energy Level Scheme

Phosphorescence and Photoconductivity

There are two main types of phosphorescence, in one the delay of the emisson is due to the time an electron spends in the luminescence center in an excited state. The second type is due to an electron spending time in a trap. The first type typically lasts on the order of milliseconds while the second type can last many hours or even days. It can be concluded that the high temperature phosphorescence observed in the Insaco sample is due to the type involving traps.

It was found that the phosphorescence decays could easily be fit to a single first order process, an exponential function. This indicates that one trap is the major contributor to the emission. The probability K of an electron escaping from a trap of depth E at temperature T is of the form:

$$K = K_o \, EXP(-E/k_b T)$$

the intensity, I, is given by:

$$I = I_o \, EXP(-tK)$$

where K_o and I_o are constants and k_b is Boltzmann's constant. If this is the proper description of what is causing the observed phosphorescence it should be possible to plot the lifetimes obtained from the data being fit to a first order process on semilogarithmic graph paper with lifetime plotted on the logarithmic scale and the inverse of the temperature on the other scale. This type of plot should result in a straight line. A plot of this type is shown in Figure 25, the dots are the lifetimes. The line in Figure 25 is seen to fit the data very well,

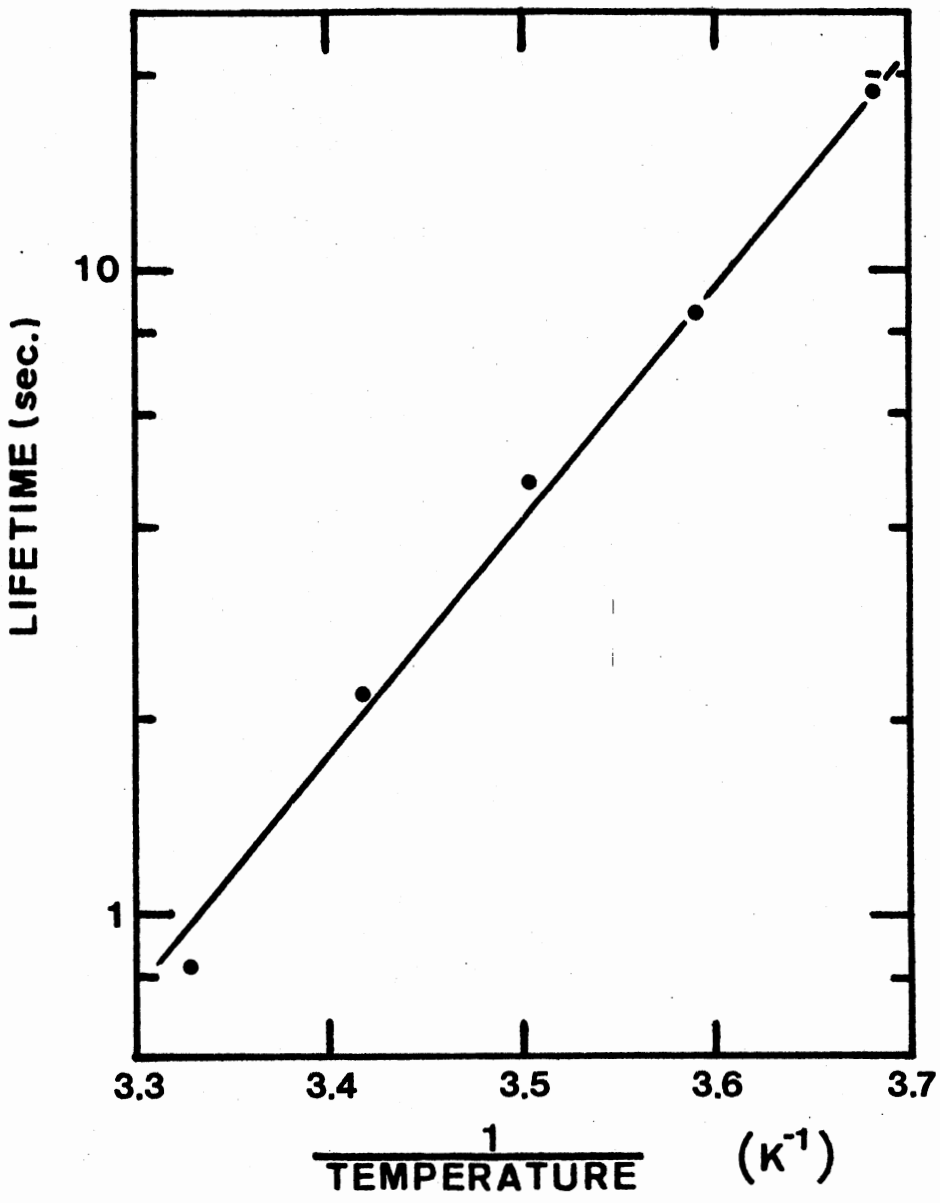

Figure 25. Semilogarithmic Plot of Lifetime Versus the Inverse of the Temperature for the Insaco Phosphorescence Data

indicating that the process suggested is correct. The slope of the line gives a trap depth of 0.72 eV ± 0.01 eV, with this K_o is found to be 1.2×10^{12} sec^{-1}.

The attention now turns to the photoconductivity experimental results. The decays observed in the photoconductivity experiments were also found to be first order and temperature dependent in a manner similar to the phosphorescence lifetimes. This indicates that the two processes might be similar. To demonstrate that they are similar a semilogarithmic plot of lifetime versus the inverse of the temperature is shown in Figure 26, where the dots are the lifetimes. The data is seen to easily be fit to a straight line, the slope of which yields a trap depth of 0.73 ± 0.01 eV. K_o is found to be 2.5×10^{12} sec^{-1}. These values are in very good agreement with those for the phosphorescence data. This not only indicates that the two processes are similar but that they are in fact the same process with a trap depth of about 0.72 eV and a K_o of magnitude 10^{12} sec^{-1}. This K_o is close to the same order of magnitude as the thermal vibrational frequency of a crystal (10^{13} sec^{-1}). This makes K_o appear to be high which at this time can not be explained.

It appears that the high temperature phosphorescence and photoconductivity in the Insaco sample both originate from traps of depth 0.72 eV. The reason this phosphorescence and photoconductivity is observed only in the Insaco sample is not at the present understood. There is no obvious difference between the Insaco sample and the Crystal Systems sample that could account for such a large effect as was observed in the Insaco sample. This might be an area for further research.

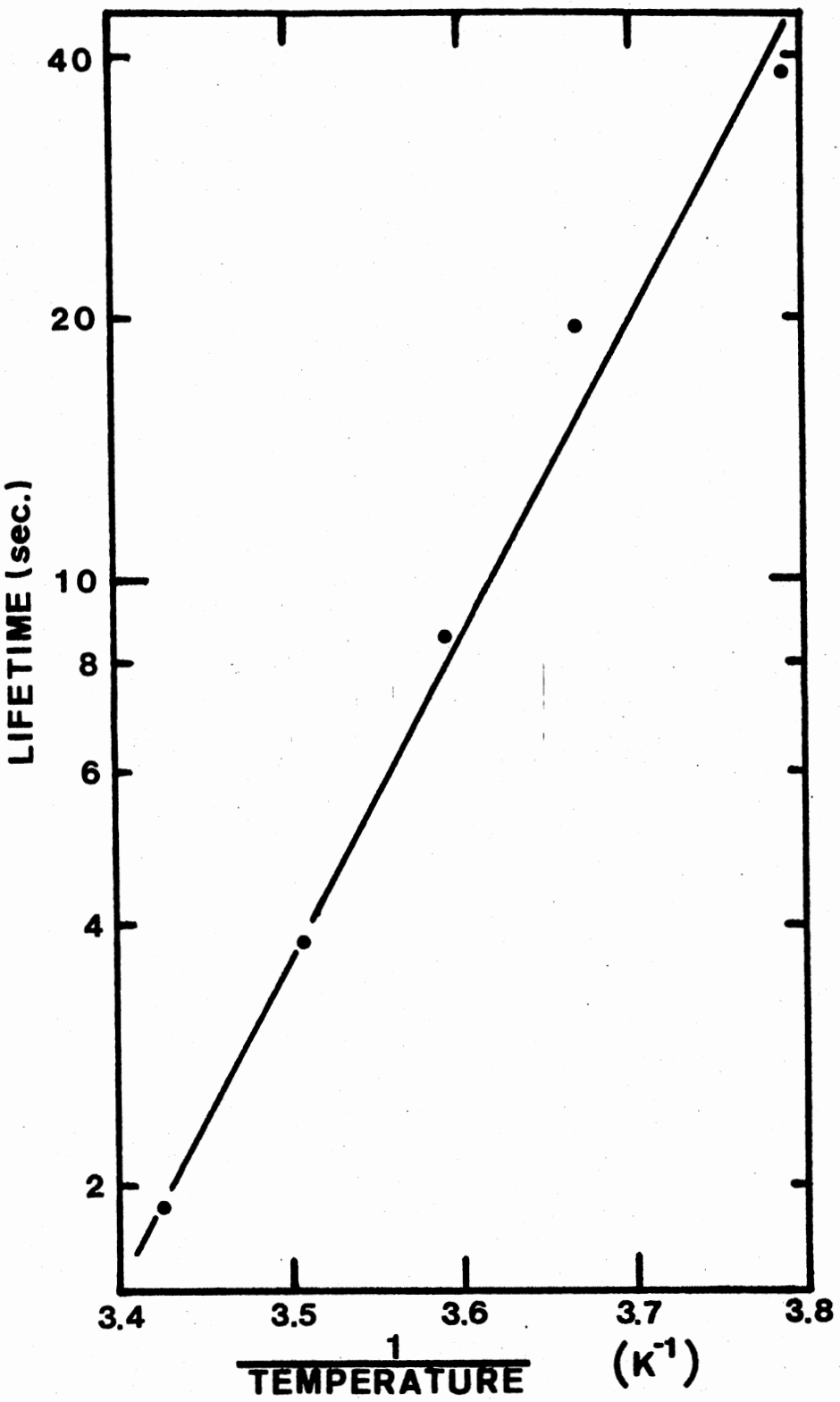

Figure 26. Semilogarithmic Plot of Lifetime Versus the Inverse of the Temperature for the Insaco Photoconductivity Data

A SELECTED BIBLIOGRAPHY

1. Summary of Properties: Synthetic Sapphire (Adolf Meller Co.).

2. Arnold, G. W., and W. D. Compton, Phys. Rev. Lett. 4, 66 (1960).

3. Pells, G. P., U.K.A.E.A. Harwell Publication, AERE-R 9359 (1979).

4. Turner, T. J., and J. H. Crawford, Solid State Commun. 17, 167 (1975).

5. Turner, T. J., and J. H. Crawford, Phys. Rev. B 13, 1736 (1976).

6. Lee, K. H., and J. H. Crawford, Jr., Phys. Rev. B 15, 4065 (1977).

7. Draeger, B. G., and G. P. Summers, Phys. Rev. B 19, 1172 (1979).

8. La, S. V., R. H. Bartram, and R. T. Cox, J. Phys. Chem. Solids 34, 1079 (1973).

9. Evans, B. D., and M. Stapelbroek, Phys. Rev. B 18, 7089 (1978).

10. Lee, K. H., and J. H. Crawford, Phys. Rev. B 19, 3217 (1979).

11. Lehman, H. W., and Hs. H. Gunthard, J. Phys. Chem. Solids 25, 941 (1964).

12. Draeger, Billy Gene, Jr., "Photoconductivity and Luminescence in Al_2O_3", 10 (Unpub. M.S. thesis, Oklahoma State University, 1975).

13. Summers, G. P. (private communication) (1979).

VITA[2]

Joel Dean Brewer

Candidate for the Degree of

Master of Science

Thesis: AN EXPERIMENTAL INVESTIGATION OF LOW TEMPERATURE FLUORESCENCE IN SAPPHIRE

Major Field: Physics

Biographical:

Personal Data: Born in Stillwater, Oklahoma, January 28, 1956, the son of Mr. and Mrs. Warren Brewer.

Education: Graduated from Coyle Public High School, Coyle, Oklahoma, in May, 1974; received the Bachelor of Science degree in Physics from Oklahoma State University in May, 1978; completed requirements for Master of Science degree at Oklahoma State University in December, 1979.